Pilowski LS, Kerwin RW, Murray RM (1993). Schizophrenia: a neuro-developmental perspective. *Neuropsychopharmacology* **9**, 83–91.

Qiao H, Noda Y, Kamei H, Nagai T, *et al.* (2001). Clozapine, but not haloperidol, reverses social behavior deficit in mice during withdrawal from chronic phencyclidine treatment. *Neuroreport* **12**, 11–15.

Raman IM, Tong G, Jahr CE (1996). Beta-adrenergic regulation of synaptic NMDA receptors by cAMP-dependent protein kinase. *Neuron* **16**, 415–421.

Rao VR, Finkbeiner S (2007). NMDA and AMPA receptors: old channels, new tricks. *Trends in Neurosciences* **30**, 284–291.

Scheetz AJ, Constantine-Paton M (1994). Modulation of NMDA receptor function: implications for vertebrate neural development. *Journal of the Federation of American Societies for Experimental Biology* **8**, 745–752.

Scott DB, Blanpied TA, Ehlers MD (2003). Coordinated PKA and PKC phosphorylation suppresses RXR-mediated ER retention and regulates the surface delivery of NMDA receptors. *Neuropharmacology* **45**, 755–767.

Shen S, Lang B, Nakamoto C, Zhang F, *et al.* (2008). Schizophrenia-related neural and behavioral phenotypes in transgenic mice expressing truncated Disc1. *Journal of Neuroscience* **28**, 10893–10904.

Slikker Jr. W, Paule MG, Wright LK, Patterson TA, Wang C (2007). System biology approaches for toxicology. *Journal of Applied Toxicology* **27**, 201–217.

Theiler K (1989). *The House Mouse – Atlas of Embryonic Development*. New York, USA: Springer-Verlag.

Wang C, McInnis J, Ross-Sanchez M, Shinnick-Gallagher P, *et al.* (2001). Long-term behavioral and neurodegenerative effects of perinatal phencyclidine administration: implications for schizophrenia. *Neuroscience* **107**, 535–550.

Watanabe M, Inoue Y, Sakimura K, Mishina M (1992). Developmental changes in distribution of NMDA receptor channel subunit mRNAs. *Neuroreport* **3**, 1138–1140.

Yanai J, Avraham Y, Levy S, Maslaton J, *et al.* (1992). Alterations in septohippocampal cholinergic innervations and related behaviors after early exposure to heroin and phencyclidine. *Brain Research Developmental Brain Research* **69**, 207–214.

0022-3565/09/3311-14–22$20.00
THE JOURNAL OF PHARMACOLOGY AND EXPERIMENTAL THERAPEUTICS

JPET 331:14–22, 2009

Vol. 331, No. 1
154724/3512655
Printed in U.S.A.

Matrix Metalloprotease-9 Inhibition Improves Amyloid β-Mediated Cognitive Impairment and Neurotoxicity in Mice[S]

Hiroyuki Mizoguchi, Kazuhiro Takuma, Emiko Fukuzaki, Daisuke Ibi, Eiichi Someya, Ko-hei Akazawa, Tursun Alkam, Hiroko Tsunekawa, Akihiro Mouri, Yukihiro Noda, Toshitaka Nabeshima, and Kiyofumi Yamada

Laboratory of Neuropsychopharmacology, Division of Life Sciences, Graduate School of Natural Science and Technology, Kanazawa University, Kanazawa, Japan (H.M., K.T., E.F., D.I., E.S., K.A., K.Y.); Futuristic Environmental Simulation Center, Research Institute of Environmental Medicine, Nagoya University, Nagoya, Japan (H.M.); Laboratory of Medicinal Pharmacology, Graduate School of Pharmaceutical Sciences, Osaka University, Osaka, Japan (K.T.); Department of Neuropsychopharmacology and Hospital Pharmacy, Nagoya University Graduate School of Medicine, Nagoya, Japan (D.I., T.A., H.T., A.M., K.Y.); Division of Clinical Science in Clinical Pharmacy Practice, Management and Research, Faculty of Pharmacy, Meijo University, Nagoya, Japan (Y.N.); and Department of Chemical Pharmacology, Graduate School of Pharmaceutical Sciences, Meijo University, Nagoya, Japan (T.N.)

Received April 7, 2009; accepted July 7, 2009

ABSTRACT

In Alzheimer's disease (AD), the expression of matrix metalloproteases (MMPs), which are capable of degrading extracellular matrix proteins, is increased in the brain. Previous studies with cultured glial cells have demonstrated that amyloid β (Aβ) protein can induce the expression of MMPs, which could be involved in the degradation of Aβ. In the present study, we investigated the role of MMP-2 and MMP-9 in cognitive impairment induced by the injection of Aβ in mice. The intracerebroventricular injection of Aβ25-35, Aβ1-40, and Aβ1-42, but not Aβ40-1, transiently increased MMP-9, but not MMP-2, activity and protein expression in the hippocampus. Immunohistochemistry revealed the expression of MMP-9 to be increased in both neurons and glial cells in the hippocampus after Aβ treatment. The Aβ-induced cognitive impairment in vivo as well as neurotoxicity in vitro was significantly alleviated in MMP-9 homozygous knockout mice and by treatment with MMP inhibitors. These results suggest the increase in MMP-9 expression in the hippocampus to be involved in the development of cognitive impairment induced by Aβ1-40. Thus, specific inhibitors of MMP-9 may have therapeutic potential for the treatment of AD. Our findings suggest that, as opposed to expectations based on previous findings, MMP-9 plays a causal role in Aβ-induced cognitive impairment and neurotoxicity.

This study was supported in part by Grants-in-Aid for Scientific Research [Grants 18790052, 19390062]; the 21st Century Center of Excellence Program from the Ministry of Education, Culture, Sports, Science and Technology of Japan; a grant from the Smoking Research Foundation, Japan; the Mochida Memorial Foundation for Medical and Pharmaceutical Research; the Suzuken Memorial Foundation; the Kanzawa Medical Research Foundation; the Japan Society for the Promotion of Science and Korea Science and Engineering Foundation under the Japan-Korea Basic Scientific Cooperation Program; the Academic Frontier Project for Private Universities; matching fund subsidy from Ministry of Education, Culture, Sports, Science and Technology [Grant 2007-2011]; and the Research on Risk of Chemical Substances, Health and Labor Science Research grants supported by the Ministry of Health, Labor and Welfare.

Article, publication date, and citation information can be found at http://jpet.aspetjournals.org.

doi:10.1124/jpet.109.154724.

[S] The online version of this article (available at http://jpet.aspetjournals.org) contains supplemental material.

Alzheimer's disease (AD), the most common neurodegenerative disorder in humans, is characterized by deterioration of cognitive and mental functions, including learning and memory. The formation of extracellular deposits of amyloid β (Aβ) peptide, leading to the formation of neuritic plaques and neurofibrillary tangles in the cortex and hippocampus, is a prominent pathological feature of AD (Yamada and Nabeshima, 2000; Selkoe and Schenk, 2003). Aβ, a spontaneously aggregating peptide of 39 to 43 amino acids, is the primary protein component of senile plaques, a pathological hallmark of AD (Hardy and Selkoe, 2002; Takuma et al., 2005a). Neurotoxicity mediated by Aβ has been well demonstrated both in vivo and in vitro and has been shown to involve oxidative stress, the perturbation of intracellular cal-

ABBREVIATIONS: AD, Alzheimer's disease; Aβ, amyloid β; AAV/Aβ, a viral vector carrying Aβ cDNA; MMP, matrix metalloprotease; LTP, long-term potentiation; MK-801, 5*H*-dibenzo[*a*,*d*]cyclohepten-5,10-imine (dizocilpine maleate); GM6001, *N*-[(2*R*)-2-(hydroxamidocarbonylmethyl)-4-methylpentanoyl]-L-tryptophan methylamide; NORT, novel-object recognition test; FITC, fluorescein isothiocyanate; PBS, phosphate-buffered saline; NeuN, neuron-specific nuclear antigen; GFAP, glial fibrillary acidic protein; LDH, lactate dehydrogenase; ANOVA, analysis of variance; NMDA, *N*-methyl-D-aspartate.

cium homeostasis, and the activation of an apoptotic pathway (Takuma et al., 2005a).

In animal experiments, we have demonstrated that the intrahippocampal injection of Aβ, including Aβ1-40, Aβ1-42, and Aβ25-35, induces hippocampal damage, learning, and memory deficits (Yamada et al., 2005; Alkam et al., 2007; Wang et al., 2007), and impairment of the cholinergic system, which play important roles in cognitive deficits associated with aging and neurodegenerative diseases (Yamada et al., 1999; Tran et al., 2001). A recent study has shown that intraventricular infusion of Aβ1-42 induces learning deficits in 9-month-old but not 2.5-month-old mice, and these learning deficits are shown 12, but not 6, weeks after infusion of Aβ1-42 in 9-month-old mice, suggesting that Aβ infusion results in age-dependent and delayed learning deficits without role of Aβ deposition and inflammation (Malm et al., 2006). In addition, we have shown that the oral administration of a viral vector carrying Aβ cDNA (AAV/Aβ) reduced the amount of Aβ accumulated and attenuated cognitive impairment in Tg2576 mice, suggesting AAV/Aβ to be safe and effective for the treatment of AD and that the accumulation of Aβ is the event initiating the decades-long pathological cascade leading to the disease (Mouri et al., 2007). Whereas plaques and amyloid fibrils have been viewed by some as resistant to proteolytic degradation, it is possible that certain proteases contribute to endogenous mechanisms leading to the clearance of plaques.

Matrix metalloproteinases (MMPs) function to remodel the pericellular environment, primarily through the cleavage of extracellular matrix proteins and cell surface components (Yong et al., 2001). Gelatinases (MMP-2 and MMP-9) are capable of cleaving collagen IV and V, laminin, and chondroitin sulfate proteoglycan, which are associated with cell adhesion (Yong et al., 2001). Furthermore, MMP-9 degrades Aβ and amyloid plaques (Yan et al., 2006) and has been implicated specifically in cerebral ischemia (Lo et al., 2002), kainate-induced neuronal injury (Szklarczyk et al., 2002), hippocampal long-term potentiation (LTP) and memory (Nagy et al., 2006), and methamphetamine dependence (Mizoguchi et al., 2007a,b). Thus, gelatinases are involved in neuronal activity-dependent synaptic plasticity and cell death in the brain.

It is interesting that MMP-9 is increased in the brains of AD patients (Backstrom et al., 1996). Moreover, MMP-9 expression in astrocytes is induced in the presence of Aβ peptide (Deb et al., 2003). MMP-9 is expressed in the cytoplasm of neurons, neurofibrillary tangles, senile plaques, and vascular walls in brain tissue from AD patients (Asahina et al., 2001). Although MMP-9 has been found to cleave the Aβ peptide at several sites (Backstrom et al., 1996; Yan et al., 2006), its potential role in Aβ-induced cognitive dysfunction and neurotoxicity has not yet been elucidated.

In the present study, we investigated the role of MMP-2 and MMP-9 in cognitive impairment induced by the intracerebroventricular injection of Aβ in mice, as well as Aβ-induced neurotoxicity in primary cultured neurons. Our findings suggest that, as opposed to expectations based on previous findings, MMP-9 plays a causal role in Aβ-induced cognitive impairment and neurotoxicity.

Materials and Methods

Animals. Male ICR mice (6 weeks old; Charles River Japan, Yokohama, Japan), weighing 20 ± 5 g at the beginning of the experiments, were used. We also used MMP-9 homozygous knockout [MMP-9(−/−)] mice and wild-type (FVB/N) mice (10–12 weeks old) obtained from The Jackson Laboratory (Bar Harbor, ME).

All experiments were performed in accordance with the Guidelines for Animal Experiments of the Kanazawa University (Kanazawa, Japan) and Nagoya University Graduate School of Medicine (Nagoya, Japan), the Guiding Principles for the Care and Use of Laboratory Animals approved by the Japanese Pharmacological Society (Tokyo, Japan), and the National Institutes of Health *Guide for the Care and Use of Laboratory Animals* (National Institutes of Health, Bethesda, MD).

Drugs. The doses of all drugs are expressed as those of the salt. Aβ25-35, Aβ1-40, and Aβ40-1 (Bachem California, Torrance, CA) were dissolved in distilled water at a concentration of 1 mg/ml and stored at −30°C before use and incubated for aggregation at 37°C for 4 days before the injection. Aβ peptides were injected intracerebroventricular at a volume of 3 μl. Vehicle and Aβ40-1 were injected as the control. All peptides were injected as described previously (Alkam et al., 2007; Wang et al., 2007). In brief, a microsyringe with a 28-gauge stainless steel needle 3.0 mm long was used for all experiments. Mice were anesthetized lightly with ether, and the needle was inserted unilaterally 1 mm to the right of the midline point equidistant from each eye, at an equal distance between the eyes and the ears and perpendicular to the plane of the skull. A single shot of the same volume (3 μl) of peptide or vehicle was delivered gradually within 3 min. Mice exhibited normal behavior within 1 min after the injection. MK-801 (Sigma-Aldrich, St. Louis, MO) at a dose of 0.1 to 0.3 mg/kg was given 30 min before Aβ25-35. GM6001 (Calbiochem, San Diego, CA) at a dose of 5 μg was intracerebroventricularly injected with Aβ in a total volume of 5 μl.

Novel-Object Recognition Test. The NORT was carried out as described previously (Mizoguchi et al., 2008). The experimental apparatus consisted of a Plexiglas open-field box (30 × 30 × 35 cm high), with a sawdust-covered floor. The apparatus was located in a sound-attenuated room and was illuminated with a 20-W bulb.

In a standard procedure, the NORT consisted of three sessions: habituation, training, and retention. Each mouse was individually habituated to the box, with 10 min of exploration in the absence of objects for two consecutive days (habituation session, days 1–2). During the training session, two novel objects were symmetrically fixed to the floor of the box, 8 cm from the walls, and each animal was allowed to explore in the box for 10 min (day 3). The objects were constructed from a golf ball, wooden column, and wall socket, which were different in shape and color but similar in size. An animal was considered to be exploring the object when its head was facing the object or it was touching or sniffing the object. The time spent exploring each object was recorded. After training, mice were immediately returned to their home cages. During the retention sessions, the animals were placed back into the same box 24 h after the training session (day 4), but one of the familiar objects used during training had been replaced with a novel object. The animals were then allowed to explore freely for 5 min, and the time spent exploring each object was recorded. Throughout the experiments, the objects were used in a counterbalanced manner in terms of their physical complexity and emotional neutrality. A preference index in the retention session, a ratio of the amount of time spent exploring the novel object over the total time spent exploring both objects, was used to measure cognitive function. In the training session, the preference index was calculated as a ratio of the time spent exploring the object that was replaced by the novel object in the retention session, over the total exploring time.

Repeated Training NORT. The procedure of repeated training NORT is the same with the standard NORT, except that the number of training sessions was increased from one to four, and then the

mice were subjected to the retention session. During the four training sessions (days 3–4, twice a day), mice were repeatedly exposed to the same two objects in the test box. During the retention session (day 5), one of the two familiar objects used during four training sessions was replaced with a novel object.

Gel Zymography. Samples were prepared as described previously (Mizoguchi et al., 2007a,b). In brief, brain tissues were homogenized in lysis buffer (50 mM Tris-HCl, 150 mM NaCl, 5 mM $CaCl_2$, 0.05% Brij 35, and 0.02% NaN_3, pH 7.6) with 1% Triton X-100 and centrifuged at 12,000*g* for 10 min to pellet insoluble material. The protein concentration in the supernatant was determined using a Protein Assay Rapid kit (Bio-Rad, Osaka, Japan). The supernatant was incubated with gelatin-Sepharose 4B (GE Healthcare, Chalfont St. Giles, Buckinghamshire, UK) that had been washed three times with the lysis buffer, with constant shaking, for 24 h at 4°C. After centrifugation at 500*g* for 2 min, the pellet was resuspended in 500 μl of the lysis buffer and washed three times. The pellet was resuspended in 150 μl of lysis buffer containing 10% dimethyl sulfoxide and shaken for 2 h, and then it was used for assaying gelatinase activity of MMP-2 and MMP-9.

The samples were subjected to electrophoresis in a 10% SDS-polyacrylamide gel electrophoresis containing 0.1% gelatin under nonreducing conditions. Gels were washed twice for 30 min in 2.5% Triton X-100 to remove SDS, washed for 30 min in incubation buffer (50 mM Tris-HCl, 5 mM $CaCl_2$, 2 μM $ZnCl_2$, 200 mM NaCl, and 0.02% Briji 35, pH 7.4) at room temperature, and further incubated for 24 h in the same buffer at 37°C. Gels were then stained for 3 h in Coomassie Blue (1% Coomassie Brilliant Blue G-250, 30% methanol, and 10% acetic acid) and destained in 40% methanol/7% acetic acid until clear bands of gelatinolysis occurred on a dark background. Total activity including pro-MMP activity was analyzed with the ATTO Densitograph Software Library Lane Analyzer (Atto Instruments, Tokyo, Japan).

Western Blotting. Brain tissues were homogenized in lysis buffer (20 mM Tris-HCl, 100 mM NaCl, 1 mM $CaCl_2$, and 0.005% Brij 35, pH 7.4) and microwaved for 15 s according to the protocol for immunoblotting with monoclonal antibodies. The homogenate was centrifuged at 13,000*g* for 30 min to pellet insoluble material. The protein concentration in the supernatant was determined using a Protein Assay Rapid kit. The sample was boiled in 2× sample buffer (0.25% bromphenol blue, 12% 2-mercaptothanol, 20% glycerol, 4% SDS, and 0.1 M Tris-HCl, pH 6.8) and subjected to SDS-polyacrylamide gel electrophoresis on a 4% stacking gel and 8% separating gel, and then transferred electrophoretically to a polyvinylidene difluoride membrane (Millipore, Billerica, MA). The same concentration (20–40 μg) of protein per lane was loaded for all Western blotting. The band intensities of the film were analyzed by densitometry. The amount of MMP-9 was calculated versus the amount of β-actin protein. The primary polyclonal rabbit or goat antibodies used in the present study were anti-MMP-9 (1:1000; Abcam plc, Cambridge, UK) and β-actin (1:2000; Santa Cruz Biotechnology, Inc., Santa Cruz, CA). The secondary antibodies, horseradish peroxidase-linked anti-rabbit and anti-goat IgG, were used at 1:2000 and 1:5000 dilutions, respectively (Kirkegaard and Perry Laboratories, Gaithersburg, MD). Immunoreactive materials on the membrane were detected using enhanced chemiluminescence Western blotting detection reagents (GE Healthcare) and exposed to X-ray film. The band intensities of the film were analyzed by densitometry.

In Situ Zymography. Mice were intracardially perfused with ice-cold saline before being frozen at −80°C using optimal cutting temperature compound (Sakura Finetechnical, Tokyo, Japan). The brains were sectioned at 20 μm in a cryostat. We adapted an in situ zymography method to localize net gelatinolytic activity in brain sections as described previously (Szklarczyk et al., 2002; Mizoguchi et al., 2007b). Nonfixed sections were incubated for 24 h at 37°C in a humid dark chamber with a reaction buffer containing 0.5 M Tris-HCl, 1.5 M NaCl, 50 mM $CaCl_2$, and 2 mM sodium azide, pH 7.6, and 100 μg/ml FITC-labeled DQ-gelatin (Invitrogen, Carlsbad, CA) intramolecularly quenched. After the incubation, sections were washed in PBS, fixed in 4% paraformaldehyde, and mounted on slides. Some sections were incubated with the broad-spectrum MMP inhibitor 1,10-*O*-phenanthroline (1 mM; Invitrogen). Samples were observed with an FITC filter, and the images were analyzed using an AxioVision 3.0 system (Carl Zeiss, Jena, Germany). The cleavage of gelatin-FITCs by tissue gelatinases releases quenched fluorescence representative of net proteolytic activity. Sections incubated without FITC-labeled DQ-gelatin were not fluorescent.

Double Immunostaining. Polyclonal rabbit anti-MMP-9 antibody (1:250; Abcam plc), monoclonal mouse anti-neuron-specific nuclear antigen (NeuN) antibody (1:200; Millipore Bioscience Research Reagents, Temecula, CA), anti-glial fibrillary acidic protein (GFAP) antibody (1:200; Millipore Bioscience Research Reagents), and anti-F8/40 antibody (1:100; Sigma-Aldrich) served as primary antibodies. Affinity-purified FITC-conjugated goat anti-rabbit IgG and rhodamine-conjugated goat anti-mouse IgG served as secondary antibodies. Samples were observed with an AxioVision 3.0 system.

Neuronal Cultures. Cortical neurons were prepared from mouse embryos at 17 days of gestation as described previously (Takuma et al., 2005b). In brief, slices of cerebral cortex were digested with trypsin and triturated in Neurobasal medium containing 2% B27 supplement, 0.5 mM glutamine, and 4.4 mM sodium bicarbonate at 4°C. Cells were separated from debris and diluted in 1 ml of the medium. After centrifugation for 2 min, the cell pellet was resuspended in Neurobasal medium containing 2% B27 supplement, 0.5 mM glutamine, 50 U/ml penicillin, and 50 μg/ml streptomycin, and plated at 2×10^6 cells/ml into 24-well plates coated with 50 μg/ml poly(D-lysine).

Aβ1-40 (Peptide Institute Inc., Osaka, Japan) at a concentration of 10 μM was added to cultured cortical neurons from ICR mice for 24 h. Cells were fixed with 3% paraformaldehyde in PBS(−) at 4°C and washed three times. Polyclonal rabbit anti-MMP-9 antibody and monoclonal mouse anti-NeuN antibody served as primary antibodies in 1% bovine serum albumin and 0.1% Triton X-100 in PBS(−). Affinity-purified FITC-conjugated goat anti-rabbit IgG and rhodamine-conjugated goat anti-mouse IgG served as secondary antibodies. Samples were observed with an AxioVision 3.0 system and LSM 510 confocal microscope (Carl Zeiss).

Cell Death Assay. Cell death was evaluated by measuring lactate dehydrogenase (LDH) activity released into the medium using a colorimetric assay as described previously (Takuma et al., 2005b). In brief, cells in 96-well plates were exposed to experimental treatments, and then 50 μl of culture supernatant was collected from each well. Supernatants were reacted with a tetrazolium salt at room temperature for 30 min, and stop solution was added. Absorbance at 405 nm was measured on a Benchmark microplate reader (Bio-Rad). Total cellular LDH activity was determined by lysing the cells. The amount of LDH activity released from cells was expressed as a percentage of total LDH activity.

An MMP-2/-9 inhibitor II (Calbiochem) at doses of 10 and 30 μM was added to the culture medium 30 min before treatment with Aβ1-40 at a dose of 10 μM in cultured cortical neurons from ICR mice. Three or 5 days after treatment, the amount of LDH released from the cultured neurons was measured. Total cellular LDH activity was determined by lysing the cells. The amount of LDH activity released from the cells was expressed as a percentage of total LDH activity.

Statistical Analysis. All data are expressed as the mean ± S.E. Statistical significance was determined using a one-way analysis of variance (ANOVA), followed by the Student-Newman-Keuls test for multigroup comparisons. p values less than 0.05 were taken to indicate statistically significant differences. Student's t test was used for two-group comparisons.

Results

Dose- and Time-Dependent Changes in MMP-9 Activity in the Hippocampus after Intracerebroventricular Injection of Aβ25-35 or Aβ1-40 in Mice. We investigated whether MMP-2 and MMP-9 activities were induced by the intracerebroventricular injection of Aβ25-35 and Aβ1-40 using gel zymography method. In Fig. 1A, lane 8 represents a zymographic control marker, murine recombinant MMP-9, whose molecular mass is approximately 105 kDa. The injection of Aβ25-35 transiently and dose-dependently increased MMP-9, but not MMP-2, activity in the hippocampus compared with the activity in the vehicle-treated control group [$F_{(2,22)} = 0.84, p > 0.05$ (Fig. 1B); $F_{(2,22)} = 7.58, p < 0.05$ (Fig. 1C) by one-way ANOVA]. MMP-9 activity was markedly increased to 500 to 1300% of control levels on day 1, but it returned to the basal levels on days 3 and 7 after injection. Likewise, the intracerebroventricular injection of Aβ1-40 dose-dependently increased MMP-9, but not MMP-2, activity in the hippocampus [$F_{(4,33)} = 0.25$, $p > 0.05$ (Fig. 2B); $F_{(4,33)} = 3.22, p < 0.05$ (Fig. 2C) by one-way ANOVA] on day 1. Again, the MMP-9 activity returned to the basal levels of vehicle or Aβ40-1-injected mice on days 3 and 7 ($p < 0.05$ by t test; Fig. 2F). It should be noted that the injection of Aβ25-35 and Aβ1-40 produced a lower molecular weight band that may be an active form of MMP-9 (Figs. 1A and 2, A and D). Moreover, the intracerebroventricular injection of Aβ1-40 tended to increase MMP-9, but not MMP-2, activity in the frontal cortex on day 1, but the change was not statistically significant (Supplemental Fig. 1). It was confirmed that the intracerebroventricular injection of the more fibrinogenic Aβ1-42 at 900 pmol significantly increased MMP-9 activity in the hippocampus on day 1 after injection [vehicle-injected control mice (n = 6), 100 ± 27; Aβ1-42-injected mice (n = 8), 460 ± 57]. The injection of Aβ1-42 also induced a minimal increase in MMP-2 activity [vehicle-injected control mice (n = 6), 100 ± 5; Aβ1-42-injected mice (n = 8), 120 ± 4].

Spatial Changes in Net Proteolytic Activity in the Hippocampus after Intracerebroventricular Injection of Aβ1-40. We analyzed the spatial changes in gelatinase

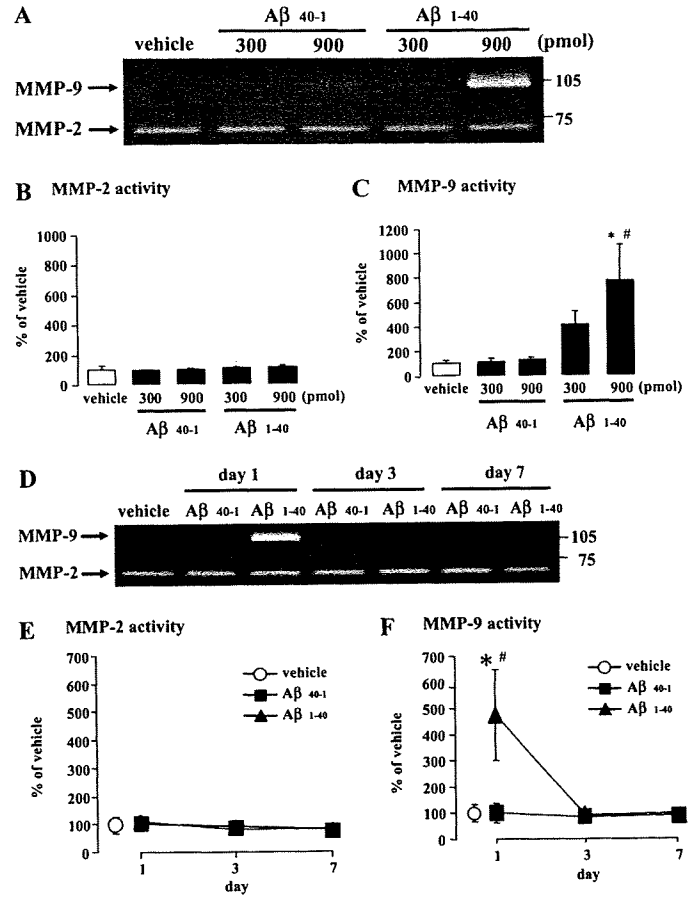

Fig. 2. Effect of intracerebroventricular injection of Aβ1-40 on MMP-2 (B and E) and MMP-9 (C and F) activities in the hippocampus. A and D, gel zymography. Mice were injected with either vehicle or Aβ1-40 at a dose of 300 or 900 pmol and then killed on day 1, 3, and 7 after the injection. Values are the mean ± S.E. [B and C; vehicle, n = 8; Aβ40-1 (300 pmol), n = 4; Aβ40-1 (900 pmol), n = 8; Aβ1-40 (300 pmol), n = 9; Aβ1-40 (900 pmol), n = 9; E and F, vehicle, n = 11; Aβ40-1 (900 pmol; day 1), n = 12; Aβ40-1 (900 pmol; day 3) n = 4; Aβ40-1 (900 pmol; day 7), n = 4; Aβ1-40 (900 pmol; day 1), n = 13; Aβ1-40 (900 pmol; day 3), n = 4; Aβ1-40 (900 pmol; day 7), n = 4]. *, $p < 0.05$ versus vehicle-injected mice. #, $p < 0.05$ versus Aβ40-1-injected mice (day 1).

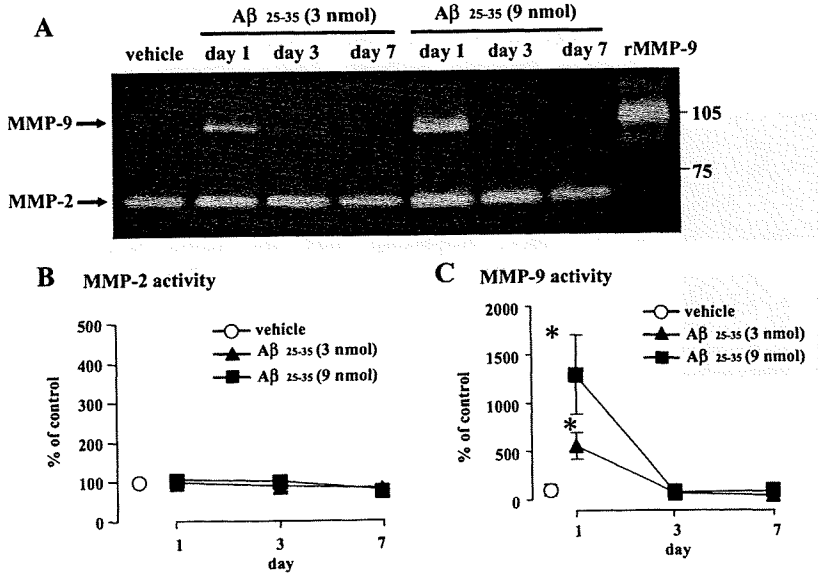

Fig. 1. Effect of intracerebroventricular injection of Aβ25-35 on MMP-2 (B) and MMP-9 (C) activities in the hippocampus. A, gel zymography. Mice were injected with either vehicle or Aβ25-35 at a dose of 3 or 9 nmol and then killed on day 1, 3, and 7 after the injection. Values are the mean ± S.E [vehicle; n = 9; Aβ25-35 (3 nmol; day 1), n = 8; Aβ25-35 (3 nmol; day 3), n = 5; Aβ25-35 (3 nmol; day 7), n = 3; Aβ25-35 (9 nmol; day 1), n = 8; Aβ25-35 (9 nmol; day 3), n = 4; Aβ25-35 (9 nmol; day 7), n = 3]. *, $p < 0.05$ versus vehicle-injected mice.

activity in the hippocampus after the intracerebroventricular injection of Aβ1-40 by in situ zymography. Brain sections were incubated with gelatin conjugated to a quenched fluorescence dye, and the cleavage of gelatin by gelatinase results in an increase in fluorescence. The signal was completely inhibited by the zinc chelator phenantroline, a broad-spectrum MMP inhibitor, indicating that the fluorescence is associated with MMP activity (Supplemental Fig. 2, compare B with A). In vehicle- and Aβ40-1-injected groups, gelatinase activity was observed in the CA1–CA4 layers and dentate gyrus of the hippocampus, indicating that constitutive gelatinolytic activity was localized to the main neuronal layers of the hippocampus. Twenty-four hours after the intracerebroventricular injection of Aβ1-40, an intense signal was visualized in the hippocampus compared with the Aβ40-1-injected group (Supplemental Fig. 2, compare D with C). In addition, the gelatinase activity was markedly increased in the molecular layer of the hippocampus in the Aβ1-40-treated group compared with the Aβ40-1-injected group (Supplemental Fig. 2, E and F).

The Intracerebroventricular Injection of Aβ1-40 Increases MMP-9 Protein Expression in the Brain. Next, we examined whether MMP-9 protein levels were also increased in the hippocampus by the intracerebroventricular injection of Aβ1-40 on day 1. A Western blot analysis revealed the hippocampal protein level to be increased 24 h after Aβ1-40 was injected at 900 pmol compared with levels in the vehicle- and Aβ40-1-treated groups [$F_{(2,15)} = 5.55, p < 0.05$ (Fig. 3A) by one-way ANOVA].

To determine the cell types in which the expression of MMP-9 is induced by the injection of Aβ1-40, double immunostaining for MMP-9 with NeuN, a neuronal marker (Fig. 3D); F4/80, a microglial marker (Fig. 3E); or GFAP, an astroglial marker (Fig. 3F), was performed. In the Aβ1-40-treated group, strong immunolabeling of MMP-9 was visualized in the CA3 layers of the hippocampus compared with the Aβ40-1-injected group (Fig. 3, compare B with C), in which the majority of the immunoreactivity was colocalized to NeuN-positive cells, suggesting the expression of MMP-9 in neurons. However, some MMP-9 immunoreactivity was observed in F4/80- or GFAP-positive cells in the hippocampus (Fig. 3, D–F).

Role of the Aβ-Induced Increase in MMP-9 Expression in Aβ-Induced Impairment of Recognition Memory. To examine the role of MMP-9 in Aβ1-40-induced cognitive dysfunction, we investigated the effect of GM6001, a broad-spectrum MMP inhibitor (Galardy et al., 1994; Wang and Tsirka, 2005), on Aβ1-40-induced impairment of recognition memory in the NORT. Cotreatment with GM6001 dose-dependently suppressed the Aβ1-40-induced increase in hippocampal MMP-9 activity compared with 2.5% dimethyl sulfoxide, and the effect of GM6001 (5 μg) was statistically significant [$F_{(2,16)} = 3.80, p < 0.05$ (Supplemental Fig. 3A) by one-way ANOVA]. However, GM6001 had little effect on MMP-2 activity, and there was no significant difference in activity between the 2.5% dimethyl sulfoxide-injected and GM6001-injected mice (Supplemental Fig. 3A). As shown in Supplemental Fig. 3B, the intracerebroventricular injection of Aβ1-40 significantly reduced exploratory preference for the novel object in the retention session [$F_{(3,18)} = 5.68, p < 0.05$ (Supplemental Fig. 3B) by one-way ANOVA], without affecting total exploration time in the training and retention sessions [data not shown; training: $F_{(3,18)} = 0.29, p > 0.05$ by one-way ANOVA; retention: $F_{(3,18)} = 2.05, p > 0.05$ by one-way ANOVA], indicating the impairment of recognition memory in Aβ1-40-injected mice. Simultaneous treatment with GM6001 (5 μg) in Aβ1-40-injected mice caused a significant improvement in exploratory preference in the retention session [$F_{(3,18)} = 5.68, p < 0.05$ (Supplemental Fig. 3B) by one-way ANOVA], without affecting the exploratory preference in the training session [$F_{(3,18)} = 0.34, p > 0.05$ (Supplemental Fig. 3B) by one-way ANOVA] or total exploration time in the training or retention session [data not shown; training: $F_{(3,18)} = 0.29, p > 0.05$ by one-way ANOVA; retention: $F_{(3,18)} = 2.05, p > 0.05$ by one-way ANOVA].

In addition to the pharmacological studies, we investigated the role of MMP-9 in Aβ1-40-induced impairment of recognition memory using MMP-9(−/−) mice. In the standard (one-training) procedure of NORT, the exploratory preference to the novel object in the retention session was markedly reduced in MMP-9(−/−) mice (49.3 ± 2.9; $n = 10$) compared with wild-type mice (69.0 ± 2.3; $n = 10$) without a change in total exploration time in the training and retention sessions. Thus, it was difficult to assess the Aβ-induced memory impairment in MMP-9(−/−) mice in a standard one-training NORT. Accordingly, the number of training sessions was increased from one to four, and the mice were subjected to the retention session (repeated training NORT). There was no difference in total exploration time in the first and fourth training sessions between Aβ40-1-treated wild-type and MMP-9(−/−) mice, respectively [first training: $F_{(3,21)} = 2.28$, $p > 0.05$ by one-way ANOVA; fourth training: $F_{(3,21)} = 1.75$, $p > 0.05$ by one-way ANOVA] (Fig. 4A). As shown in Fig. 4B, there was no difference in exploratory preference in the retention session between Aβ40-1-treated wild-type and MMP-9(−/−) mice, indicating that the Aβ40-1-treated MMP-9(−/−) mice could recognize the novel object 24 h after four training sessions [$F_{(3,21)} = 17.9, p < 0.05$ by one-way ANOVA for retention] (Fig. 4B). Under these conditions, Aβ1-40-injected wild-type mice showed a marked impairment of exploratory preference in the retention session [$F_{(3,21)} = 17.9, p < 0.05$ by one-way ANOVA] (Fig. 4B), without exhibiting a change in exploratory preference in the training sessions [first training: $F_{(3,21)} = 2.00, p > 0.05$ by one-way ANOVA; fourth training: $F_{(3,21)} = 1.99, p > 0.05$ by one-way ANOVA] (Fig. 4B) or in total exploration time in the training sessions [first training: $F_{(3,21)} = 2.28, p > 0.05$ by one-way ANOVA;

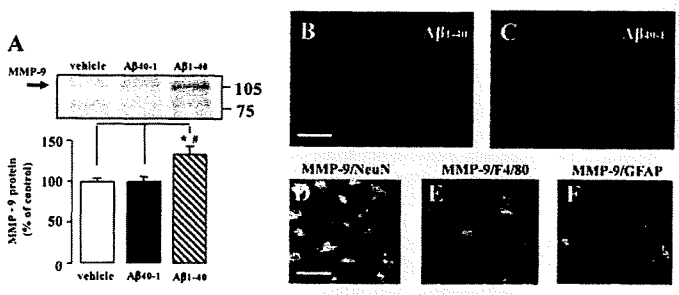

Fig. 3. Effect of intracerebroventricular injection of Aβ1-40 on the MMP-9 protein level in the hippocampus. A, Western blot analysis: Mice were injected with either vehicle, Aβ40-1, or Aβ1-40 at a dose of 900 pmol and then killed 1 day later. Values are the mean ± S.E. (A; $n = 6$). *, $p < 0.05$ versus vehicle-injected mice. #, $p < 0.05$ versus Aβ40-1-injected mice. B to F, double immunostaining for MMP-9 (B–F; green) and NeuN (D; red), F4/80 (E; red), or GFAP (F; red) in the CA3 layer of the hippocampus. Scale bar, 100 μm (B) and 10 μm (D).

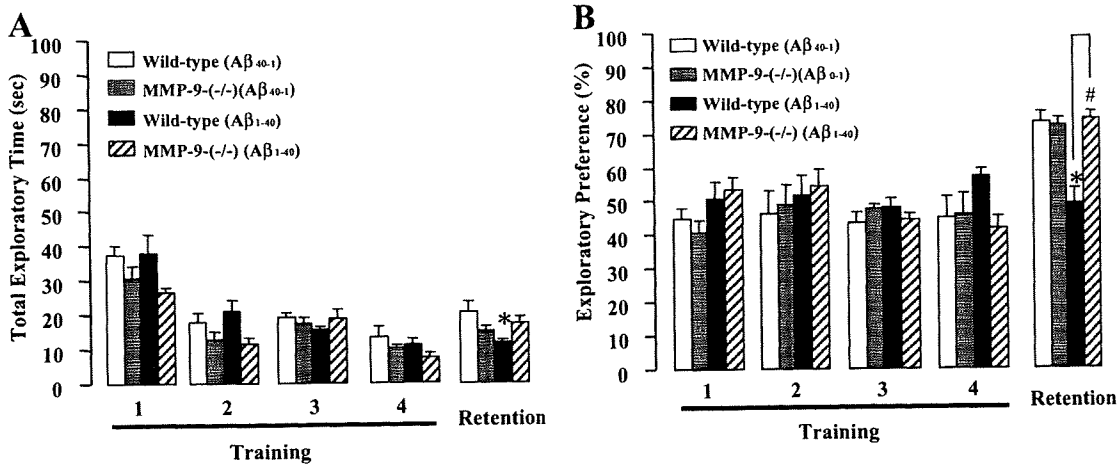

Fig. 4. Effect of Aβ1-40 on total exploratory time (A) and exploratory preference (B) in repeated training NORT in wild-type and MMP-9(−/−) mice. Mice were intracerebroventricularly injected with Aβ1-40 at a dose of 900 pmol. Values are the mean ± S.E. (n = 5–7). *, $p < 0.05$ versus wild type (Aβ40-1). #, $p < 0.05$ versus wild type (Aβ1-40).

fourth training: $F_{(3,21)} = 1.75$, $p > 0.05$ by one-way ANOVA] (Fig. 4A). There was a slight but significant difference in total exploration time in the retention session between Aβ40-1- and Aβ1-40-injected wild-type mice [$F_{(3,21)} = 4.86$, $p < 0.05$ by one-way ANOVA] (Fig. 6A).

Pretreatment with MK-801 Inhibits Aβ25-35-Induced Increase in MMP-9 Expression and Impairment of Recognition Memory. To examine the mechanism by which Aβ injection induces the MMP expression, we investigated the effect of MK-801, a noncompetitive *N*-methyl-D-aspartate (NMDA) receptor antagonist, on the Aβ25-35-induced increase in MMP-9 expression and impairment of recognition memory in the NORT. Pretreatment with MK-801 had no effect on the hippocampal MMP-9 activity in vehicle-treated mice. However, the NMDA receptor antagonist completely inhibited the Aβ25-35-induced increase in MMP-9 expression in the hippocampus [$F_{(3,15)} = 6.17$, $p < 0.05$ by one-way ANOVA] (Fig. 5A). Moreover, pretreatment with MK-801 (0.1–0.3 mg/kg) in Aβ25-35-injected mice caused a dose-dependent and significant improvement of exploratory preference in the retention session [$F_{(5,51)} = 2.74$, $p < 0.05$ by one-way ANOVA] (Fig. 5B), without affecting exploratory preference in the training session [$F_{(5,51)} = 0.65$, $p > 0.05$ by one-way ANOVA] (Fig. 5B) or total exploration time in the training [$F_{(5,51)} = 0.93$, $p > 0.05$ by one-way ANOVA] or retention session [$F_{(5,51)} = 0.87$, $p > 0.05$ by one-way ANOVA]. Post hoc analysis indicated that MK-801 at 0.3 mg/kg, but not 0.1 mg/kg, significantly improved exploratory preference in Aβ25-35-treated mice ($p < 0.05$). MK-801 at 0.1 to 0.3 mg/kg in the vehicle-treated control group had no effect on exploratory preference or total exploration time in the training and retention sessions (Fig. 5B).

Effect of Aβ1-40 on MMP-9 Expression in Primary Cultured Cortical Neurons. Treatment with Aβ1-40 (Supplemental Fig. 4E), but not Aβ40-1 (Supplemental Fig. 4C), at a dose of 10 μM for 24 h induced MMP-9 expression in primary cultured cortical neurons compared with vehicle treatment (Supplemental Fig. 4A). Immunoreactivity was observed in NeuN-positive cells, indicating that Aβ1-40 treatment can induce MMP-9 expression in neurons (Supplemental Fig. 4G). NeuN-positive cells differed between the Aβ1-40- (Supplemental Fig. 4F) and Aβ40-1-treated (Supplemental Fig. 4D) groups, suggesting that cell death was not induced drastically 24 h after Aβ1-40 treatment (Supplemental Fig. 4, compare F with D).

A Specific Inhibitor of MMP-2/-9 Attenuated Aβ1-40-Induced Neurotoxicity in Primary Cultured Cortical Neurons. Finally, we investigated the role of MMP-9 in Aβ1-40-induced neurotoxicity by measuring LDH activity released into the culture medium. Aβ1-40 treatment for 3 or 5 days markedly induced the release of LDH from cultured cortical neurons [3 days (Fig. 6A): $F_{(5,18)} = 17.6$, $p < 0.05$ by one-way ANOVA; 5 days (Fig. 6B): $F_{(5,18)} = 40.4$, $p < 0.05$ by one-way ANOVA]. However, cotreatment with rather specific MMP-2/-9 inhibitor reduced the amount of LDH released from cultured cortical neurons [3 days (Fig. 6A): $F_{(5,18)} = 17.6$, $p < 0.05$ by one-way ANOVA; 5 days (Fig. 6B): $F_{(5,18)} =$

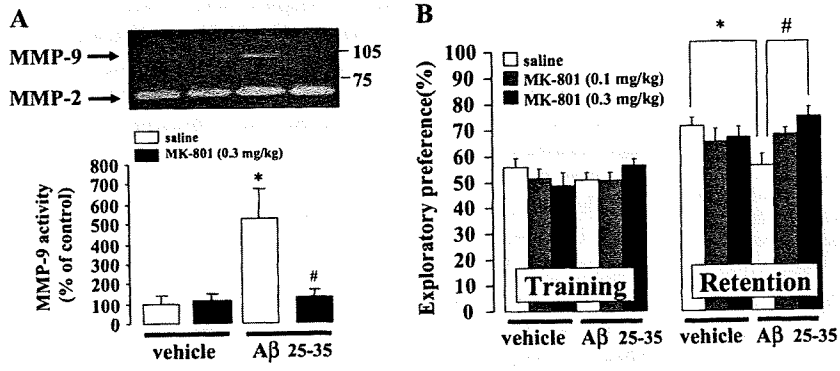

Fig. 5. Effect of MK-801 on Aβ25-35-induced increase in hippocampal MMP-9 activity (A) and memory impairment (B). Mice were given MK-801 at 0.1 to 0.3 mg/kg 30 min before receiving an intracerebroventricular injection of Aβ25-35 at 3 nmol. Values are the mean ± S.E. (n = 4–5 for A; n = 9–10 for B). *, $p < 0.05$ versus saline + vehicle. #, $p < 0.05$ versus saline + Aβ25-35.

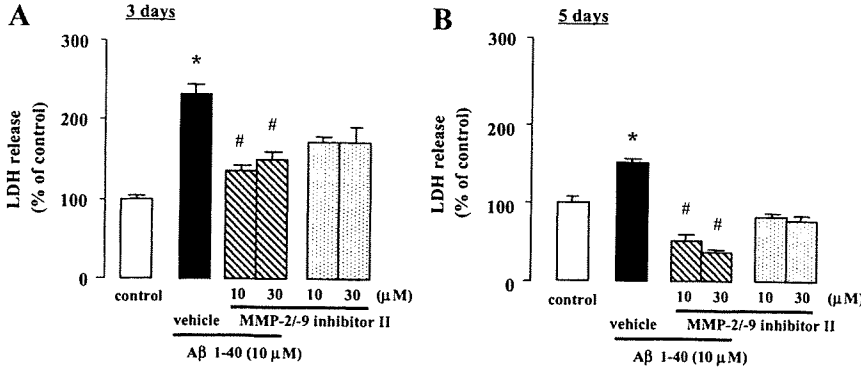

Fig. 6. Effect of a specific MMP-2/-9 inhibitor on Aβ-induced neurotoxicity in primary cultured cortical neurons. A, MMP-2/-9 inhibitor II at a dose of 10 or 30 μM was added simultaneously with Aβ1-40 at a dose of 10 μM to primary cultured cortical neurons from ICR mice. Three or 5 days later, the amount of LDH released from cultured neurons was measured. Total cellular LDH activity was determined by lysing the cells. The amount of LDH activity released from the cells was expressed as a percentage of total LDH activity. Values are the mean ± S.E. for four determinations per experimental condition. *, $p < 0.05$ versus control. #, $p < 0.05$ versus Aβ1-40 + vehicle.

40.4 $p < 0.05$ by one-way ANOVA], although the inhibitor itself had no effect on the release.

In addition to the pharmacological studies, we investigated the role of MMP-9 in Aβ1-40-induced neurotoxicity in primary cultured neurons from MMP-9(−/−) mice. Treatment with Aβ1-40 at 10 μM for 5 days markedly increased the amount of LDH released from cultured cortical neurons of wild-type mice [$F_{(5,20)} = 3.47$, $p < 0.05$ by one-way ANOVA] (Fig. 7). The Aβ1-40-induced release was almost completely suppressed in the neurons from MMP-9(−/−) mice compared with those from wild-type mice (Fig. 7).

Discussion

In the Aβ25-35-, Aβ1-40-, and Aβ1-42-injected mice, MMP-9 activity and protein expression were transiently increased in the hippocampus. We demonstrated using inhibitors of MMPs and MMP-9(−/−) mice that the increase in MMP-9 expression in the hippocampus is associated with the development of cognitive impairment and neurotoxicity induced by Aβ. Thus, specific inhibitors of MMP-9 may have a therapeutic potential for the treatment of AD.

Members of the MMP subfamily, the gelatinases MMP-2 and MMP-9, are initially expressed as inactive proenzymes and cleaved into active forms after cellular release (Van den Steen et al., 2002); this property places these proteases in a unique position to regulate levels of substrates in the extracellular space. Our present study apparently indicated that the activity of MMP-2 was constantly expressed, whereas that of MMP-9 was very weak in the hippocampus of vehicle-injected mice. The intracerebroventricular injection of Aβ led to a transient induction of MMP-9 expression in the hippocampus. In addition, we demonstrated that the Aβ-induced expression of MMP-9 was localized to neuronal and glial cells in the hippocampus. Previous study has revealed that both MMP-2 and MMP-9 are expressed in the presence of Aβ (Deb and Gottschall, 1996) and highly expressed and secreted by astrocytes (Muir et al., 2002; Deb et al., 2003). In contrast, MMP-9 is synthesized in neurons of the human hippocampus (Backstrom et al., 1996) and is expressed in the cytoplasm of neurons, neurofibrillary tangles, vascular walls, and senile plaques in the brain tissues of AD patients (Asahina et al., 2001). Our findings are consistent with these previous reports.

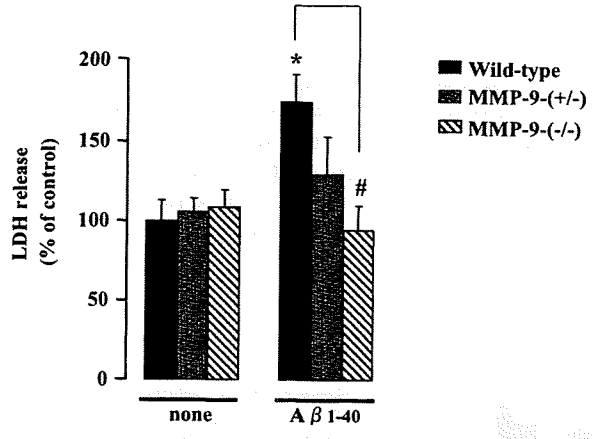

Fig. 7. Aβ-induced neurotoxicity in primary cultured cortical neurons from MMP(−/−) mice. Primary cultured cortical neurons from wild-type, MMP-9(+/−), or MMP-9(−/−) mice were treated with Aβ (10 μM). Five days later, the amount of LDH released from cultured neurons was measured. Total cellular LDH activity was determined by lysing the cells. The amount of LDH activity released from the cells was expressed as a percentage of total LDH activity. Values are the mean ± S.E. for three to five determinations per experimental condition. *, $p < 0.05$ versus control. #, $p < 0.05$ versus Aβ1-40 + vehicle.

To clarify the mechanism underlying Aβ-induced expression of MMP-9, we focused on the role of NMDA receptors, because it has been reported that Aβ activates NMDA receptors (Snyder et al., 2005), and MMP-9 expression is induced via NMDA receptors (Meighan et al., 2006; Nagy et al., 2006; Tian et al., 2007). Pretreatment with MK-801 inhibited the Aβ-induced increase in MMP-9 expression and cognitive impairment, indicating that MMP-9's induction and cognitive dysfunction are induced by Aβ treatment associated at least in part with the activation of NMDA receptors in this model. In fact, an excessive amount of glutamate in the synaptic microenvironment and the persistent influx of Ca^{2+} through NMDA receptors are considered major causes of neurodegeneration in AD (Wenk, 2006). For example, in the rat magnocellular nucleus basalis, Aβ-induced toxicity was effectively reduced by MK-801, and Aβ promoted an excitotoxic pathway that includes astroglial depolarization, extracellular glutamate accumulation, NMDA receptor activation culminating in intracellular Ca^{2+} overload, and cell death (Harkany et al., 2000). Direct injection of Aβ1-40 in the hippocampus caused neuronal loss in the CA1 area and treatment with an NMDA antagonist, memantine, reduced the Aβ-induced neuronal degeneration (Miguel-Hidalgo et al., 2002) as well as working memory deficits (Yamada et al., 2005). These findings support the hypothesis that NMDA receptors play a central role in Aβ-induced neurotoxicity. In addition, the expression and activity of MMP-9 depend on the activation of NMDA receptors and are associated with the development of LTP (Meighan et al., 2006; Nagy et al., 2006). The activation of NMDA receptors promotes the development of dendritic

spines through MMP-mediated cell adhesion molecules (Tian et al., 2007). Together with our findings that Aβ treatment increased MMP-9 expression in primary cultured neurons, the activation and expression of MMP-9 are directly and/or indirectly regulated by Aβ through the activation of NMDA receptors in neuronal cells.

MMP-9 might be induced as a protection to destroy the plaques and amyloid fibrils. The growing list of proteases can degrade soluble Aβ in vitro, namely, neprilysin (Howell et al., 1995), insulin-degrading enzyme (Kurochkin and Goto, 1994), and MMP-9 (Yan et al., 2006), suggesting a role for these proteases in regulating endogenous basal levels of Aβ in vivo. Notably, MMP-9 was reported to cleave insoluble Aβ in vitro (Yan et al., 2006). The view of the function of MMPs in the long-lasting synaptic plasticity is expanding, and evidence suggests that MMP-9 is up-regulated and becomes proteolytically active selectively during the maintenance phase of LTP at CA3-CA1 synapses in the hippocampus (Nagy et al., 2006), and similar findings have been recently made in rat prefrontal cortex. These reports suggest that MMPs function in cellular processes that contribute to learning and memory. Therefore, although we assumed that MMP inhibitors potentiate the Aβ-induced cognitive dysfunction and neurotoxicity, our findings do not support such an assumption. In Supplemental Fig. 3, we showed that MMP inhibitor treatment ameliorated Aβ-induced impairment of recognition memory, suggesting that the transient increase in hippocampal MMP-9 activity is functionally associated with the development of Aβ-induced cognitive deficits. The findings made with a pharmacological inhibitor were further supported by the result that the intracerebroventricular injection of Aβ1-40 impaired recognition memory in wild-type but not MMP-9(−/−) mice. Accordingly, even if MMP-9 can degrade Aβ/plaques, it may randomly and nonselectively destroy the extracellular matrix and neural membranes, leading to neuronal dysfunction and cognitive impairment.

Recent evidence has linked MMPs to various pathological conditions in the central nervous system, including ischemia, multiple sclerosis, Parkinson's disease, and malignant glioma. This implies that, in addition to its known function to degrade extracellular macromolecules, MMP may serve as a mediator that leads to apoptotic and/or necrotic cell death. In fact, recent studies indicate that MMP-9 has direct neurotoxic effects. Jourquin et al. (2003) demonstrated the increased release and activity of MMP-9 after stimulation with neurotoxic kainate in organotropic cultures and reduced neuronal cell death by the inhibition of MMP-9. Conversely, incubation with recombinant MMP-9 induced neuron death in the organotropic cultures. Alternatively, MMP-3 is reported to play a major role in degenerative human brain disorders such as Parkinson' disease (Kim et al., 2005). In the present study, MMP inhibitor II, reported to be highly selective for MMP-2 and MMP-9 (Tamura et al., 1998), blocked the Aβ-induced release of LDH, indicating that MMP-9 is crucial in Aβ-induced neuronal cell death. Genetic evidence also showed that Aβ-induced neurotoxicity was markedly reduced in primary cultured cortical neurons from MMP-9(−/−) mice compared with those from wild-type mice (Fig. 7). However, there is a report that GM6001, a broad-spectrum metalloproteinase inhibitor, acts synergistically with Aβ to enhance neurotoxicity in cultured neurons (Ethell et al., 2002). The discrepancy may reflect differences in the cell death assay and the specificity of inhibitors used because GM6001 can inhibit all MMPs and a-disintegrin-and-a-metalloproteinases.

In conclusion, we have demonstrated for the first time that MMP-9 activity and protein expression are transiently increased in the hippocampus by the intracerebroventricular injection of Aβ25-35, Aβ1−40, and Aβ1−42. We hypothesize that Aβ-induced secondary dysfunction such as MMP activation, could result in learning deficits by impairing synaptic function in the hippocampus. The present findings highlight the contribution of neural/glial MMP-9 to Aβ-induced neurotoxicity and cognitive impairment and support the case for highly selective MMP-9 inhibitors that could reduce deleterious proteolytic activity and neuronal death. Thus, specific inhibitors of MMP-9 may have therapeutic potential for the treatment of AD.

References

Alkam T, Nitta A, Mizoguchi H, Itoh A, and Nabeshima T (2007) A natural scavenger of peroxynitrites, rosmarinic acid, protects against impairment of memory induced by Abeta(25-35). *Behav Brain Res* **180**:139–145.

Asahina M, Yoshiyama Y, and Hattori T (2001) Expression of matrix metalloproteinase-9 and urinary-type plasminogen activator in Alzheimer's disease brain. *Clin Neuropathol* **20**:60–63.

Backstrom JR, Lim GP, Cullen MJ, and Tökés ZA (1996) Matrix metalloproteinase-9 (MMP-9) is synthesized in neurons of the human hippocampus and is capable of degrading the amyloid-beta peptide (1-40). *J Neurosci* **16**:7910–7919.

Deb S and Gottschall PE (1996) Increased production of matrix metalloproteinases in enriched astrocyte and mixed hippocampal cultures treated with beta-amyloid peptides. *J Neurochem* **66**:1641–1647.

Deb S, Wenjun Zhang J, and Gottschall PE (2003) Beta-Amyloid induces the production of active, matrix-degrading proteases in cultured rat astrocytes. *Brain Res* **970**:205–213.

Ethell DW, Kinloch R, and Green DR (2002) Metalloproteinase shedding of Fas ligand regulates beta-amyloid neurotoxicity. *Curr Biol* **12**:1595–1600.

Galardy RE, Cassabonne ME, Giese C, Gilbert JH, Lapierre F, Lopez H, Schaefer ME, Stack R, Sullivan M, and Summers B (1994) Low molecular weight inhibitors in corneal ulceration. *Ann N Y Acad Sci* **732**:315–323.

Hardy J and Selkoe DJ (2002) The amyloid hypothesis of Alzheimer's disease: progress and problems on the road to therapeutics. *Science* **297**:353–356.

Harkany T, Abrahám I, Timmerman W, Laskay G, Tóth B, Sasvári M, Kónya C, Sebens JB, Korf J, Nyakas C, et al. (2000) Beta-Amyloid neurotoxicity is mediated by a glutamate-triggered excitotoxic cascade in rat nucleus basalis. *Eur J Neurosci* **12**:2735–2745.

Howell S, Nalbantoglu J, and Crine P (1995) Neutral endopeptidase can hydrolyze beta-amyloid(1-40) but shows no effect on beta-amyloid precursor protein metabolism. *Peptides* **16**:647–652.

Jourquin J, Tremblay E, Décanis N, Charton G, Hanessian S, Chollet AM, Le Diguardher T, Khrestchatisky M, and Rivera S (2003) Neuronal activity-dependent increase of net matrix metalloproteinase activity is associated with MMP-9 neurotoxicity after kainate. *Eur J Neurosci* **18**:1507–1517.

Kim YS, Kim SS, Cho JJ, Choi DH, Hwang O, Shin DH, Chun HS, Beal MF, and Joh TH (2005) Matrix metalloproteinase-3: a novel signaling proteinase from apoptotic neuronal cells that activates microglia. *J Neurosci* **25**:3701–3711.

Kurochkin IV and Goto S (1994) Alzheimer's beta-amyloid peptide specifically interacts with and is degraded by insulin degrading enzyme. *FEBS Lett* **345**:33–37.

Lo EH, Wang X, and Cuzner ML (2002) Extracellular proteolysis in brain injury and inflammation: role for plasminogen activations and matrix metalloproteinases. *J Neurosci Res* **69**:1–9.

Malm T, Ort M, Tähtivaara L, Jukarainen N, Goldsteins G, Puoliväli J, Nurmi A, Pussinen R, Ahtoniemi T, Miettinen TK, et al. (2006) Beta-Amyloid infusion results in delayed and age-dependent learning deficits without role of inflammation or beta-amyloid deposits. *Proc Natl Acad Sci U S A* **103**:8852–8857.

Miguel-Hidalgo JJ, Alvarez XA, Cacabelos R, and Quack G (2002) Neuroprotection by memantine against neurodegeneration induced by beta-amyloid(1-40). *Brain Res* **958**:210–221.

Meighan SE, Meighan PC, Choudhury P, Davis CJ, Olson ML, Zornes PA, Wright JW, and Harding JW (2006) Effects of extracellular matrix-degrading proteases matrix metalloproteinases 3 and 9 on spatial learning and synaptic plasticity. *J Neurochem* **96**:1227–1241.

Mizoguchi H, Takuma K, Fukakusa A, Ito Y, Nakatani A, Ibi D, Kim HC, and Yamada K (2008) Improvement by minocycline of methamphetamine-induced impairment of recognition memory in mice. *Psychopharmacology (Berl)* **196**:233–241.

Mizoguchi H, Yamada K, Mouri A, Niwa M, Mizuno T, Noda Y, Nitta A, Itohara S, Banno Y, and Nabeshima T (2007a) Role of matrix metalloproteinase and tissue inhibitor of MMP in methamphetamine-induced behavioral sensitization and reward: implications for dopamine receptor down-regulation and dopamine release. *J Neurochem* **102**:1548–1560.

Mizoguchi H, Yamada K, Niwa M, Mouri A, Mizuno T, Noda Y, Nitta A, Itohara S, Banno Y, and Nabeshima T (2007b) Reduction of methamphetamine-induced sensitization and reward in matrix metalloproteinase-2 and -9-deficient mice. *J Neurochem* **100**:1579–1588.

Mouri A, Noda Y, Hara H, Mizoguchi H, Tabira T, and Nabeshima T (2007) Oral vaccination with a viral vector containing Abeta cDNA attenuates age-related Abeta accumulation and memory deficits without causing inflammation in a mouse Alzheimer model. *FASEB J* **21:**2135–2148.

Muir EM, Adcock KH, Morgenstern DA, Clayton R, von Stillfried N, Rhodes K, Ellis C, Fawcett JW, and Rogers JH (2002) Matrix metalloproteases and their inhibitors are produced by overlapping populations of activated astrocytes. *Brain Res Mol Brain Res* **100:**103–117.

Nagy V, Bozdagi O, Matynia A, Balcerzyk M, Okulski P, Dzwonek J, Costa RM, Silva AJ, Kaczmarek L, and Huntley GW (2006) Matrix metalloproteinase-9 is required for hippocampal late-phase long-term potentiation and memory. *J Neurosci* **26:** 1923–1934.

Selkoe DJ and Schenk D (2003) Alzheimer's disease: molecular understanding predicts amyloid-based therapeutics. *Annu Rev Pharmacol Toxicol* **43:**545–584.

Snyder EM, Nong Y, Almeida CG, Paul S, Moran T, Choi EY, Nairn AC, Salter MW, Lombroso PJ, Gouras GK, et al. (2005) Regulation of NMDA receptor trafficking by amyloid-beta. *Nat Neurosci* **8:**1051–1058.

Szklarczyk A, Lapinska J, Rylski M, McKay RD, and Kaczmarek L (2002) Matrix metalloproteinase-9 undergoes expression and activation during dendritic remodeling in adult hippocampus. *J Neurosci* **22:**920–930.

Takuma K, Yan SS, Stern DM, and Yamada K (2005a) Mitochondrial dysfunction, endoplasmic reticulum stress, and apoptosis in Alzheimer's disease. *J Pharmacol Sci* **97:**312–316.

Takuma K, Yao J, Huang J, Xu H, Chen X, Luddy J, Trillat AC, Stern DM, Arancio O, and Yan SS (2005b) ABAD enhances Abeta-induced cell stress via mitochondrial dysfunction. *FASEB J* **19:**597–598.

Tamura Y, Watanabe F, Nakatani T, Yasui K, Fuji M, Komurasaki T, Tsuzuki H, Maekawa R, Yoshioka T, Kawada K, et al. (1998) Highly selective and orally active inhibitors of type IV collagenase (MMP-9 and MMP-2): *N*-sulfonylamino acid derivatives. *J Med Chem* **41:**640–649.

Tian L, Stefanidakis M, Ning L, Van Lint P, Nyman-Huttunen H, Libert C, Itohara S, Mishina M, Rauvala H, and Gahmberg CG (2007) Activation of NMDA receptors promotes dendritic spine development through MMP-mediated ICAM-5 cleavage. *J Cell Biol* **178:**687–700.

Tran MH, Yamada K, Olariu A, Mizuno M, Ren XH, and Nabeshima T (2001) Amyloid beta-peptide induces nitric oxide production in rat hippocampus: association with cholinergic dysfunction and amelioration by inducible nitric oxide synthase inhibitors. *FASEB J* **15:**1407–1409.

Van den Steen PE, Dubois B, Nelissen I, Rudd PM, Dwek RA, and Opdenakker G (2002) Biochemistry and molecular biology of gelatinase B or matrix metalloproteinase-9 (MMP-9). *Crit Rev Biochem Mol Biol* **37:**375–536.

Wang D, Noda Y, Zhou Y, Mouri A, Mizoguchi H, Nitta A, Chen W, and Nabeshima T (2007) The allosteric potentiation of nicotinic acetylcholine receptors by galantamine ameliorates the cognitive dysfunction in beta amyloid25-35 i.c.v.-injected mice: involvement of dopaminergic systems. *Neuropsychopharmacology* **32:**1261–1271.

Wang J and Tsirka SE (2005) Neuroprotection by inhibition of matrix metalloproteinases in a mouse model of intracerebral haemorrhage. *Brain* **128:**1622–1633.

Wenk GL (2006) Neuropathologic changes in Alzheimer's disease: potential targets for treatment. *J Clin Psychiatry* **67:**3–7.

Yamada K and Nabeshima T (2000) Animal models of Alzheimer's disease and evaluation of anti-dementia drugs. *Pharmacol Ther* **88:**93–113.

Yamada K, Takayanagi M, Kamei H, Nagai T, Dohniwa M, Kobayashi K, Yoshida S, Ohhara T, Takuma K, and Nabeshima T (2005) Effects of memantine and donepezil on amyloid beta-induced memory impairment in a delayed-matching to position task in rats. *Behav Brain Res* **162:**191–199.

Yamada K, Tanaka T, Han D, Senzaki K, Kameyama T, and Nabeshima T (1999) Protective effects of idebenone and alpha-tocopherol on beta-amyloid-(1-42)-induced learning and memory deficits in rats: implication of oxidative stress in beta-amyloid-induced neurotoxicity in vivo. *Eur J Neurosci* **11:**83–90.

Yan P, Hu X, Song H, Yin K, Bateman RJ, Cirrito JR, Xiao Q, Hsu FF, Turk JW, Xu J, et al. (2006) Matrix metalloproteinase-9 degrades amyloid-beta fibrils in vitro and compact plaques in situ. *J Biol Chem* **281:**24566–24574.

Yong VW, Power C, Forsyth P, and Edwards DR (2001) Metalloproteinases in biology and pathology of the nervous system. *Nat Rev Neurosci* **2:**502–511.

Address correspondence to: Dr. Kiyofumi Yamada, Department of Neuropsychopharmacology and Hospital Pharmacy, Nagoya University Graduate School of Medicine, Showa-ku, Nagoya 466-8560, Japan. E-mail: kyamada@med.nagoya-u.ac.jp

0022-3565/09/3311-319–326$20.00
THE JOURNAL OF PHARMACOLOGY AND EXPERIMENTAL THERAPEUTICS
Copyright © 2009 by The American Society for Pharmacology and Experimental Therapeutics
JPET 331:319–326, 2009

Vol. 331, No. 1
155069/3519288
Printed in U.S.A.

Silibinin Attenuates Amyloid β_{25-35} Peptide-Induced Memory Impairments: Implication of Inducible Nitric-Oxide Synthase and Tumor Necrosis Factor-α in Mice

P. Lu, T. Mamiya, L. L. Lu, A. Mouri, M. Niwa, M. Hiramatsu, L. B. Zou, T. Nagai, T. Ikejima, and T. Nabeshima

Department of Chemical Pharmacology, Graduate School of Pharmaceutical Sciences, Meijo University, Nagoya, Japan (P.L., T.M., L.L.L., A.M., M.N., M.H., T.Nab.); China-Japan Research Institute of Medical and Pharmaceutical Sciences (P.L., T.I.) and Department of Pharmacology (L.B.Z., L.L.), Shenyang Pharmaceutical University, Shenyang, China; Division of Scientific Affairs, Japanese Society of Pharmacopoeia, Tokyo, Japan (A.M.); and Department of Neuropsychopharmacology and Hospital Pharmacy, Nagoya University, Graduate School of Medicine, Nagoya, Japan (T.Nag.)

Received April 15, 2009; accepted July 27, 2009

ABSTRACT

In Alzheimer's disease (AD), the deposition of amyloid peptides is invariably associated with oxidative stress and inflammatory responses. Silibinin (silybin), a flavonoid derived from the herb milk thistle, has potent anti-inflammatory and antioxidant activities. However, it remains unclear whether silibinin improves amyloid β (Aβ) peptide-induced neurotoxicity. In this study, we examined the effect of silibinin on the fear-conditioning memory deficits, inflammatory response, and oxidative stress induced by the intracerebroventricular injection of Aβ peptide$_{25-35}$ (Aβ_{25-35}) in mice. Mice were treated with silibinin (2, 20, and 200 mg/kg p.o., once a day for 8 days) from the day of the Aβ_{25-35} injection (day 0). Memory function was evaluated in cued and contextual fear-conditioning tests (day 6). Nitrotyrosine levels in the hippocampus and amygdala were examined (day 8). The mRNA expression of inducible nitric-oxide synthase (iNOS) and tumor necrosis factor-α (TNF-α) in the hippocampus and amygdala was measured 2 h after the Aβ_{25-35} injection. We found that silibinin significantly attenuated memory deficits caused by Aβ_{25-35} in the cued and contextual fear-conditioning test. Silibinin significantly inhibited the increase in nitrotyrosine levels in the hippocampus and amygdala induced by Aβ_{25-35}. Nitrotyrosine levels in these regions were negatively correlated with memory performance. Moreover, real-time RT-PCR revealed that silibinin inhibited the overexpression of iNOS and TNF-α mRNA in the hippocampus and amygdala induced by Aβ_{25-35}. These findings suggest that silibinin (i) attenuates memory impairment through amelioration of oxidative stress and inflammatory response induced by Aβ_{25-35} and (ii) may be a potential candidate for an AD medication.

This work was supported in part by grants-in-aid for "Academic Frontier Project for Private Universities (2007–2011) from the Ministry of Education, Culture, Sports, Science and Technology (MEXT) of Japan; Grant-in-Aid for Scientific Research (B) from MEXT of Japan [Grant 20390073]; Grant-in-Aid for Exploratory Research from Sprout Society for the Promotion of Science [Grant 19659017]; grants-in-aid for Regional Joint Research Program for Private Universities to cover current expenses from MEXT; Research Science of Pharmaceutical and Medical Devices and Research on the Risk of Chemical Substances from the Ministry of Health, Labor and Welfare (MHLW) of Japan; Research on Regulatory Science of Pharmaceutical and Medical Devices from MHLW, International Research Project Supported by the Meijo Asian Research Center; a research grant from Japan China Medical Association, Japan; and research grants from the Takeda Science Foundation, from the Uehara Memorial Foundation, and from the Nagai Foundation Tokyo.

Article, publication date, and citation information can be found at http://jpet.aspetjournals.org.

doi:10.1124/jpet.109.155069.

Alzheimer's disease (AD) is a progressive neurodegenerative disorder characterized by extraneuronal deposits of amyloid β (Aβ) peptide and the intraneuronal accumulations of hyperphosphorylated τ (Blennow et al., 2006). The deposition of Aβ in the brain is assumed to initiate a pathological cascade that results in synaptic dysfunction, synaptic loss, neuronal death, and cognitive dysfunction (Walsh and Selkoe, 2004).

The deposition of Aβ is invariably associated with oxidative stress and inflammatory response, which may contribute to neuronal dysfunction or death (Butterfield et al., 2007; Farfara et al., 2008). Abundant reactive microglia and astrocytes surround the Aβ plaques in the AD brain (Miyazono et al., 1991; McGeer et al., 2006). The activated microglia or

ABBREVIATIONS: AD, Alzheimer's disease; NO, nitric oxide; Aβ, amyloid β peptide; CMC, carboxymethylcellulose; $ONOO^-$, peroxynitrite; iNOS, inducible nitric-oxide synthase; LPS, lipopolysaccharide; RT-PCR, reverse transcription-polymerase chain reaction; silibinin, (2*R*,3*R*)-3,5,7-trihydroxy-2-[(2*R*,3*R*)-3-(4-hydroxy-3-methoxyphenyl)-2-(hydroxymethyl)-2,3-dihydrobenzo[b][1,4]dioxin-6-yl]chroman-4-one; TNF-α, tumor necrosis factor-α.

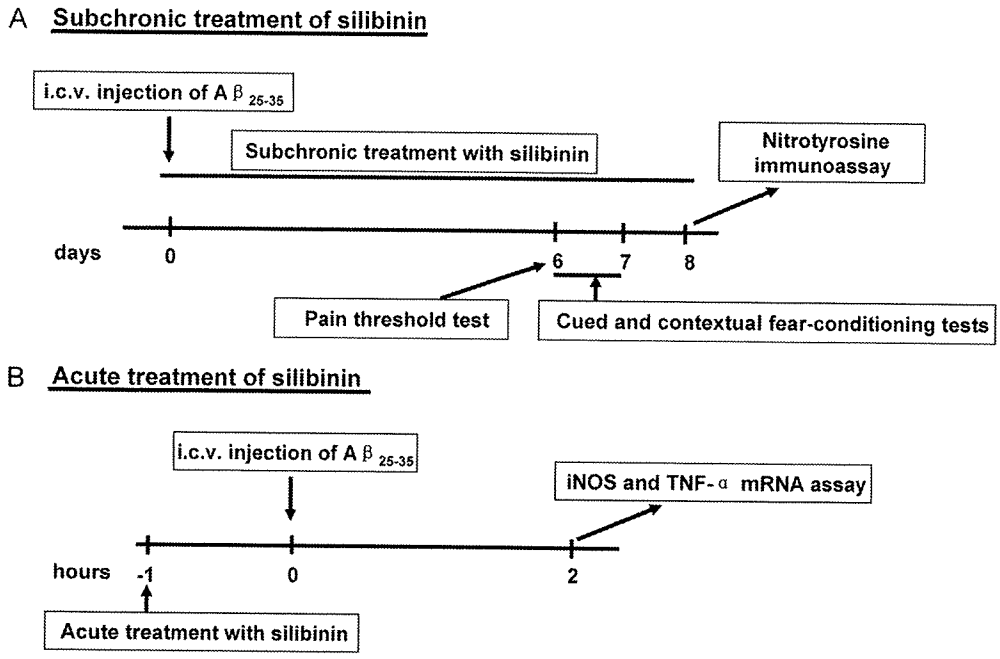

Fig. 1. The experimental design of the study showing subchronic treatment of silibinin (A) and acute treatment of a silibinin (B).

astrocytes release reactive oxygen species and proinflammatory molecules that act to exacerbate the disease process and contribute to neuronal death (Combs et al., 2001). TNF-α, a pro-inflammatory cytokine, has been shown to increase in AD patients (Fillit et al., 1991; Perry et al., 2001). Aβ-induced expression of TNF-α leads to overexpression of inducible nitric-oxide synthase (iNOS) in experimental animals (Akama and Van Eldik, 2000; Combs et al., 2001; Alkam et al., 2008). Peroxynitrite ($ONOO^-$) is one of the products formed from nitric oxide and superoxide and has a variety of chemical reactions producing compounds such as nitrotyrosine (Reiter et al., 2000; Tran et al., 2003). Interestingly, the accumulation of nitrotyrosine correlated with increased levels of cerebral Aβ and the severity of cognitive impairment (Smith et al., 1997; Ishii et al., 2000; Tran et al., 2003).

$A\beta_{25-35}$ is the core fragment of full-length Aβ and possesses many of the characteristics of the full-length Aβ peptide, including aggregative ability and neurotoxic property and is detected in the brain of AD patients (Pike et al., 1995; Kubo et al., 2002). There are reports that the intracerebroventricular administration of $A\beta_{25-35}$ peptide into rodent brain induces histological and biochemical changes, memory deficits, oxidative damage, and inflammatory responses within 1 or 2 weeks (Maurice et al., 1996; Alkam et al., 2008). Therefore, this animal model is used for screening new candidates for AD therapy worldwide.

Silibinin [(2*R*,3*R*)-3,5,7-trihydroxy-2-[(2*R*,3*R*)-3-(4-hydroxy-3-methoxyphenyl)-2-(hydroxy-methyl)-2,3-dihydrobenzo[*b*][1,4] dioxin-6-yl]chroman-4-one] is a flavonoid derived from the herb milk thistle (*Silybum marianum*) and has been reported to have anti-inflammatory and antioxidative effects (Kren and Walterová, 2005). For instance, silymarin, a mixture of flavonoids present in milk thistle, has protective effects against ethanol-induced brain injury (La Grange et al., 1999) and lipopolysaccharide (LPS)-induced neurotoxicity (Wang et al., 2002). We have reported recently that silibinin ameliorates $A\beta_{25-35}$-induced recognition memory impairment in mice (Lu et al., 2009). However, it is unclear whether silibinin ameliorates impairments of other types of memory such as fear memory and whether the inflammatory system is involved in the ameliorative effect of silibinin on Aβ-induced memory impairment. In this study, we investigated the effect of silibinin on memory impairment induced by $A\beta_{25-35}$ in cued and contextual fear-conditioning tests. We also examined its effect on changes in nitrotyrosine levels as well as TNF-α and iNOS mRNA expression in the brains of mice.

Materials and Methods

Animals. Male ICR mice (5 weeks old) were obtained from Japan SLC Inc. (Shizuoka, Japan). They were housed in plastic cages and kept in a regulated environment (23 ± 0.5°C, 50 ± 5% humidity) with a 12/12-h light/dark cycle (lights on from 8:00 AM to 8:00 PM). The mice received food (CE2; Clea Japan Inc., Tokyo, Japan) and water ad libitum. Behavioral experiments were carried out in a sound-attenuated and air-regulated experimental room, to which mice were habituated for at least 1 h. All experiments were performed in accordance with the Guidelines for Animal Experiments of the Faculty of Pharmaceutical Sciences of Meijo University and the *Guiding Principles for the Care and Use of Laboratory Animals*. The procedures involving animals and their care conformed to the international guidelines set out in the *Guide for the Care and Use of Laboratory Animals* (Institute of Laboratory Animal Resources, 1996).

Treatment. Silibinin was purchased from Panjin Green Biological Development Co., Ltd. (Panjin, Liaoning, China) and suspended in a 0.3% carboxymethylcellulose (CMC) solution. $A\beta_{25-35}$ (Bachem, Bubendorf, Switzerland) was dissolved in double-distilled water at a concentration of 1 mg/ml and stored at −20°C. $A\beta_{25-35}$ was aggregated or "aged," by incubating it in distilled water at 37°C for 4 days before the injection. $A\beta_{25-35}$ was injected intracerebroventricularly in a volume of 3 μl (3 nmol/mouse) on day 0 as in our previous report (Lu et al., 2009) (Fig. 1). Mice were anesthetized lightly with ether, and the needle was inserted unilaterally 1 mm to the right of the midline point equidistant from each eye at an equal distance between the eyes and the ears and perpendicular to the plane of the skull (anteroposterior, −0.22 mm from the bregma; lateral, 1 mm from the bregma; ventral, −2.5 mm from the skull). Mice were administered silibinin (2, 20, or 200 mg/kg/day p.o.) or the 0.3% CMC

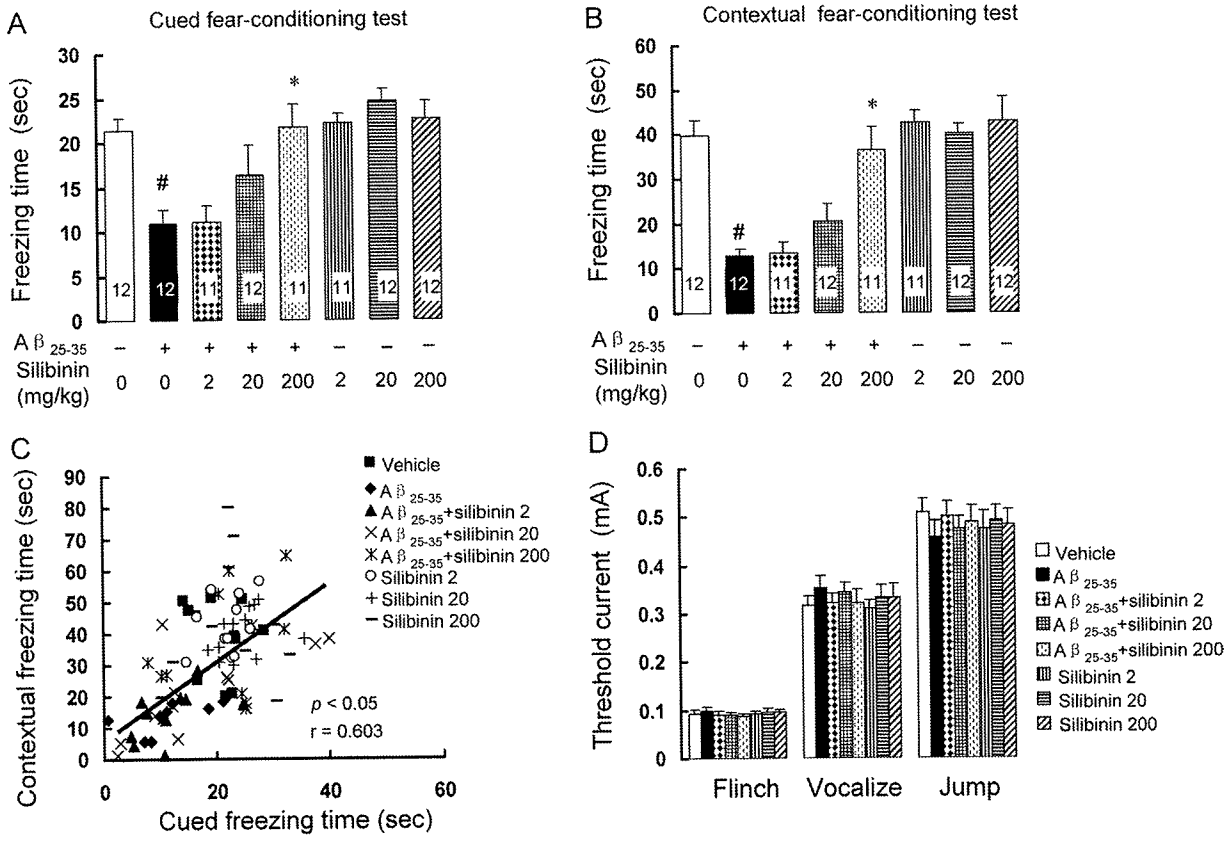

Fig. 2. Effect of silibinin on memory impairment induced by $A\beta_{25-35}$ in cued and contextual fear-conditioning tests. A, cued fear-conditioning test. B, contextual fear-conditioning test. C, correlation between cued and contextual freezing time. D, pain threshold test. Results were expressed as the mean ± S.E.M. (n = 11 or 12 and is shown in each column) and analyzed by a one-way ANOVA, followed by Tukey's test for multiple comparisons. #, $p < 0.05$ compared with CMC-treated, distilled water-injected mice; *, $p < 0.05$ compared with CMC-treated $A\beta_{25-35}$-injected mice.

solution by gavage for 8 days after the treatment with $A\beta_{25-35}$. All compounds were systemically administered in a volume of 0. 1 ml/10 g body weight.

Cued and Contextual Fear-Conditioning Tests. Cued and contextual fear-conditioning tests were carried out on days 6 and 7 (Fig. 1A) after the injection of $A\beta_{25-35}$ according to a previous report (Wang et al., 2007). For measuring basal levels of the freezing response (preconditioning phase), mice were individually placed in a neutral (uncontexual) cage (width × length × height; 23 × 23 × 12 cm) for 1 min and then in the conditioning cage (25 × 31 × 11 cm) for 2 min before the conditioning phase. For conditioning, mice were placed in the conditioning cage, and then a 15-s tone (80 dB) was delivered as a conditioned stimulus. During the last 5 s of the tone stimulus, a foot shock of 0.6 mA was delivered as an unconditioned stimulus through a shock generator (Brainscience Idea Co. Ltd, Osaka, Japan). This procedure was repeated four times with 15-s intervals. Cued and contextual tests were carried out 24 h after the fear-conditioning phase on day 7. For the cued fear-conditioning test, the freezing response was measured in a neutral cage for 1 min in the presence of a continuous tone stimulus identical to the conditioned stimulus. For the contextual fear-conditioning test, mice were placed in the conditioning cage, and the freezing response was measured for 2 min without tone and the unconditioned stimulus. A freezing response was defined as four paws of a mouse staying still and the animal stooped down.

Pain Threshold. This test was carried out on day 6 after $A\beta_{25-35}$ injection. The dark compartment of the passive avoidance apparatus was used to determine the threshold of pain from electrical stimuli. Mice were habituated to apparatus for 15 min before a series of inescapable shocks was delivered. Each series consisted of 11 shocks at the following intensities: 0.01, 0.02, 0.04, 0.06, 0.08, 0.1, 0.2, 0.3, 0.4, 0.6, and 0.8 mA. The duration of each shock was 2 s, and the shocks were delivered at 30-s intervals. Thresholds for flinch (forepaws off of the grid floor), jump (all four paws off of the grid floor), and vocalization were measured.

Western Blotting. The mice received the final administration of silibinin 1 h before decapitation on day 8 after Aβ treatment (Fig. 1A). The hippocampus and amygdala were removed on an ice-cold glass plate and stored at −80°C. Tissues were homogenized in 150 μl of ice-cold extraction buffer [20 mM Tris-HCl buffer, pH 7.6, 150 mM NaCl, 2 mM EDTA·2Na, 50 mM sodium fluoride, 1 mM sodium vanadate, 1% Nonidet P-40, 1% sodium deoxycholate, 0.1% SDS, 1 mg/ml pepstatin, 1 mg/ml aprotinin, and 1 mg/ml leupeptin]. The protein concentration of lysate was determined using a Pierce BCA Protein Assay Kit (Thermo Scientific, Rockford, IL). Equal amounts of protein (20 μg) were separated by 10% SDS-polyacrylamide gel electrophoresis and transferred electrophoretically to a polyvinylidene difluoride membrane (Millipore Corporation, Billerica, MA). It was then incubated in 5% skim milk in a washing buffer [Tris-buffered saline containing 0.05% (v/v) Tween 20] for 2 h at room temperature. The membranes were incubated with mouse anti-nitrotyrosine clone 1A6 (1:1000) (Upstate Cell Signaling, Lake Placid, NY) or mouse anti-actin primary antibody (1:1000) (Santa Cruz Biotechnology Inc., Santa Cruz, CA) at 4°C overnight. The membrane was incubated with horseradish peroxidase-labeled anti-mouse IgG (1:1000) (KPL, Gaithersburg, MD). Immunoreactive complexes on the membrane were detected using Western blotting detection reagents (GE Healthcare Bio-Sciences, Little Chalfont, Buckinghamshire, UK) according to the manufacturer's instructions and exposed to X-ray film. The intensity of each protein band on the film was analyzed with the Atto Densitograph 4.1 system (Atto, Tokyo, Japan) and corrected with the corresponding β-actin level. The results were expressed as a percentage of the control.

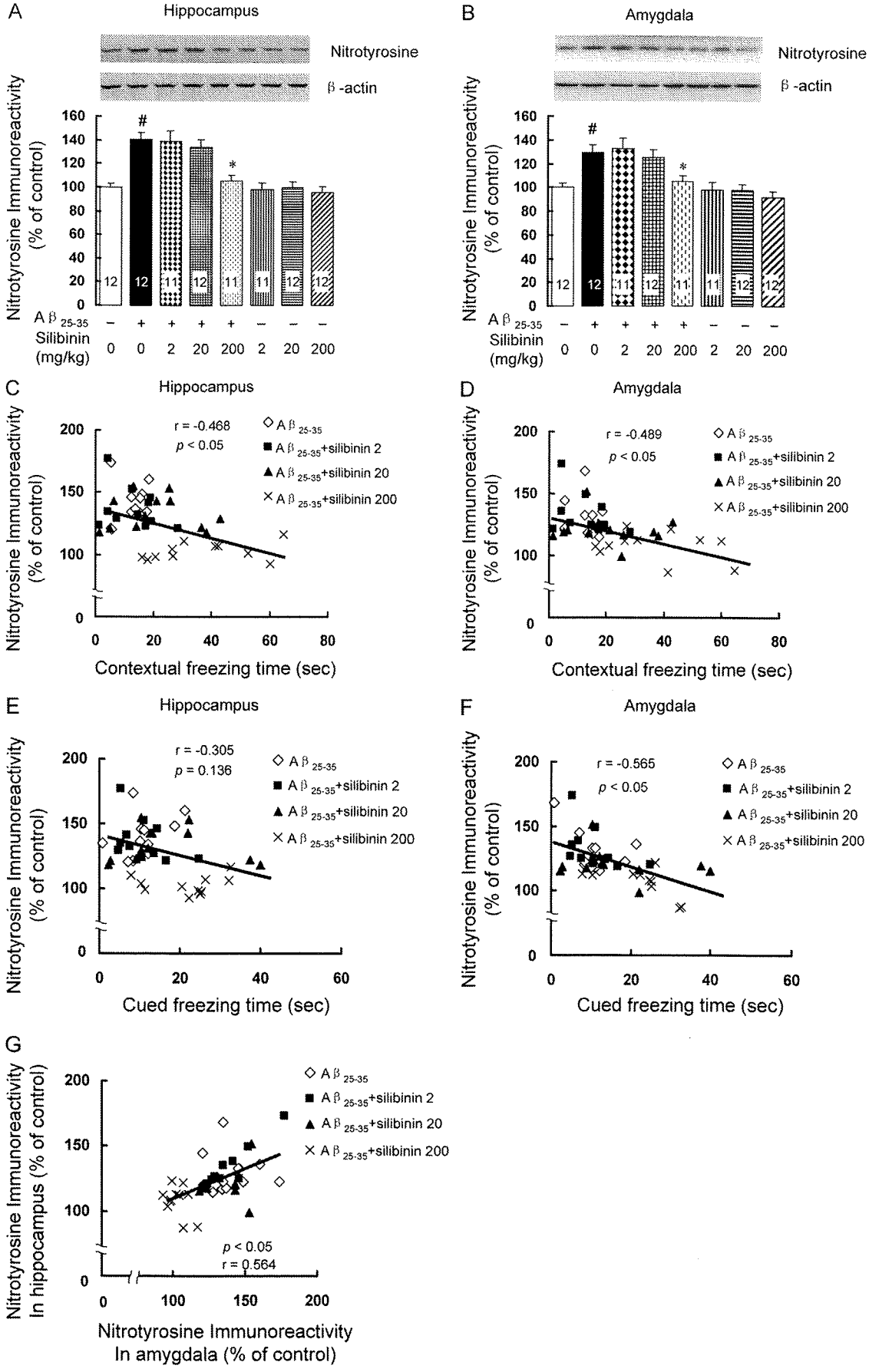

Real-Time Reverse Transcription-Polymerase Chain Reaction. Mice were treated with silibinin and $A\beta_{25-35}$ 3 and 2 h before the decapitation, respectively (Fig. 1B) because our previous report demonstrated that levels of TNF-α and iNOS mRNA peaked 2 h after $A\beta_{25-35}$ injection (Alkam et al., 2008). The hippocampus and amygdala were removed on an ice-cold glass plate and stored at −80°C. Tissues were homogenized, and total RNA was extracted using an RNeasy total RNA isolation kit (Qiagen, Valencia, CA). The primers used were as follows: for iNOS (GenBank accession number NM 010927), forward primer, 5′-GGGCAGCCTGTGAGACCTT-3′, and reverse primer, 5′-GCATTGGAAGTGAAGCGTTTC-3′; TaqMan probe, 5′-TGCGACAGCACAAGTCACAGCCCC-3′; and for TNF-α (GenBank accession number NM 023517), forward primer, 5′-CTTTCGGTTGCTCTTTGGTTGAG-3′, and reverse primer, 5′-GCAGCTCTGTCTGTTGGATCAG-3′; PCRs were performed using the One-Step SYBR PrimeScript RT-PCR kit (Takara, Kyoto, Japan). The reaction profile consisted of a first round at 95°C for 3 min and then 40 cycles of denaturation at 95°C for 10 s, annealing at 60°C for 34 s, and extension at 72°C for 1 min, with a final extension reaction carried out at 72°C for 10 min. RT-PCR was carried out with a Bio-Rad iCycler iQTM real-time PCR detection system (Bio-Rad Laboratories, Hercules, CA). Expression levels were calculated as described previously (Wada et al., 2000).

To standardize the quantification, β-actin was amplified simultaneously. The threshold cycle of each gene was determined as the PCR cycle at which there was an increase in reporter fluorescence above a baseline signals. The difference in threshold cycles between the target gene and β-actin gives the standardized expression level (delta threshold cycle, dCt). Subtraction of the dCt of distilled water-injected and CMC-treated mice from each group gives the delta delta threshold cycle (ddCt) values that were used to calculate relative expression levels in each group with the formula 2^{-ddCt}. The expression levels of each gene were expressed as the fold increase in each group compared with distilled water-injected and CMC-treated mice.

Statistical Analyses. The results are expressed as the mean ± S.E.M. Statistical significance was determined with the one-way ANOVA followed by Tukey's multiple comparisons test. A Pearson correlation analysis was performed to elucidate the relationships. $p < 0.05$ was taken as a significant level of difference.

Results

Effect of Silibinin on Memory Impairment Induced by $A\beta_{25-35}$ in Fear-Conditioning Tests. Cued and contextual fear-conditioning tests were carried out on day 6 after the injection of $A\beta_{25-35}$. In the preconditioning phase (training), mice showed less of a freezing response. There were no differences in the basal levels of freezing response in the groups [$F(7,92) = 0.763$, $p = 0.619$ in a neutral cage; $F(7,92) = 0.120$, $p = 0.997$ in the conditioning cage; data not shown]. The contextual and cued-dependent tests were performed 24 h after conditioning. $A\beta_{25-35}$-injected mice exhibited less of a cued or contextual-dependent freezing response than distilled water-injected mice (cued freezing response: $p < 0.05$, Fig. 2A; contextual freezing response: $p < 0.05$, Fig. 2B), indicating an impairment of associative memory. Silibinin dose-dependently attenuated the impairment of cued and contextual freezing responses in $A\beta_{25-35}$-injected mice [$F(7,92) = 6.799$, $p < 0.001$, Fig. 2A; $F(7,92) = 13.09$, $p < 0.001$, Fig. 2B]. Tukey's post hoc analysis revealed that silibinin at 200 mg/kg significantly attenuated the memory impairment in $A\beta_{25-35}$-injected mice ($p < 0.05$, Fig. 2A; $p < 0.05$, Fig. 2B). In addition, silibinin itself had no significant effect on either freezing response in distilled water-injected mice [$F(3,46) = 0.799$, $p = 0.501$, Fig. 2A; $F(3,46) = 0.200$, $p = 0.896$, Fig. 2B]. We also observed a correlation between cued and contextual freezing responses ($r = 0.603$, $p < 0.05$, Fig. 2C).

As shown in Fig. 2D, there were no differences among the groups in the levels of electric current required to elicit flinching [$F(7,92) = 0.309$, $p = 0.948$], vocalization [$F(7,92) = 0.369$, $p = 0.918$], and jumping [$F(7,92) = 0.243$, $p = 0.973$].

Effect of Silibinin on the Level of Nitrotyrosine. $A\beta_{25-35}$-injected mice showed a significant increase of nitrotyrosine levels in the hippocampus and amygdala compared with distilled water-injected mice [hippocampus: $F(7,92) = 15.33$, $p < 0.001$, post hoc, $p < 0.05$, Fig. 3A; amygdala: $F(7,92) = 9.165$, $p < 0.001$, post hoc, $p < 0.05$, Fig. 3B]. Silibinin significantly attenuated the increase in nitrotyrosine levels induced by $A\beta_{25-35}$ ($p < 0.05$, Fig. 3A; $p < 0.05$, Fig. 3B). Silibinin did not affect nitrotyrosine levels in the hippocampus or amygdala of distilled water-injected mice [$F(3,46) = 0.180$, $p = 0.909$, Fig. 3A; $F(3,46) = 0.328$, $p = 0.805$, Fig. 3B]. In addition, nitrotyrosine levels in the hippocampus and amygdala negatively correlated with contextual freezing responses (correlation between nitrotyrosine levels in the hippocampus and contextual freezing response: $r = -0.468$, $p < 0.05$, Fig. 3C; correlation between nitrotyrosine levels in the amygdala and contextual freezing response: $r = -0.489$, $p < 0.05$, Fig. 3D), although the negative correlation between nitrotyrosine level and cued freezing response was observed in the amygdala but not in the hippocampus (correlation between nitrotyrosine levels in the hippocampus and cued freezing response: $r = -0.305$, $p = 0.136$, Fig. 3E; correlation between nitrotyrosine levels in the amygdala and cued freezing response: $r = -0.565$, $p < 0.05$, Fig. 3F). We also found that the increase in nitrotyrosine immunoreactivity in the hippocampus induced by $A\beta_{25-35}$ correlates with that in the amygdala ($r = -0.564$, $p < 0.05$, Fig. 3G).

Effect of Silibinin on iNOS mRNA Expression. A significant increase of iNOS mRNA expression was observed in the hippocampus and amygdala of $A\beta_{25-35}$-injected mice compared with distilled water-injected mice (hippocampus: $p < 0.05$, Fig. 4A; amygdala: $p < 0.001$, Fig. 4B). Silibinin significantly attenuated the increase induced by $A\beta_{25-35}$ in the hippocampus and amygdala [$F(3,31) = 10.846$, $p < 0.001$, post hoc, $p < 0.05$, Fig. 4A; $F(3,31) = 8.345$, $p < 0.001$, post hoc, $p < 0.05$, Fig. 4B]. Silibinin did not affect iNOS mRNA expression in the hippocampus or amygdala of distilled water-injected mice ($p = 0.534$, Fig. 4A; $p = 0.864$, Fig. 4B).

Effect of Silibinin on TNF-α mRNA Expression. A significant increase of TNF-α mRNA expression was observed in the hippocampus and amygdala of $A\beta_{25-35}$-injected mice compared with distilled water-injected mice (hippocampus: $p < 0.05$, Fig. 5A; amygdala: $p < 0.05$, Fig. 5B). Silibinin

Fig. 3. Effect of silibinin on nitrotyrosine levels in the hippocampus and amygdala of $A\beta_{25-35}$-injected mice. A and B, nitrotyrosine levels in the hippocampus (A) and amygdala (B). C to F, correlation of contextual freezing time with nitrotyrosine-immunoreactivity in the hippocampus (C) or amygdala (D) and correlation of cued freezing time with nitrotyrosine immunoreactivity in the hippocampus (E) or amygdala (F). G, correlation of the nitrotyrosine immunoreactivity in the hippocampus with that in the amygdala. Results were expressed as the mean ± S.E.M. ($n = 11$ or 12 and was shown in each column) and analyzed by a one-way ANOVA, followed by Tukey's test for multiple comparisons in A and B, by Pearson correlation analysis (C to G). #, $p < 0.05$ compared with CMC-treated, distilled water-injected mice; *, $p < 0.05$ compared with CMC-treated, $A\beta_{25-35}$-injected mice.

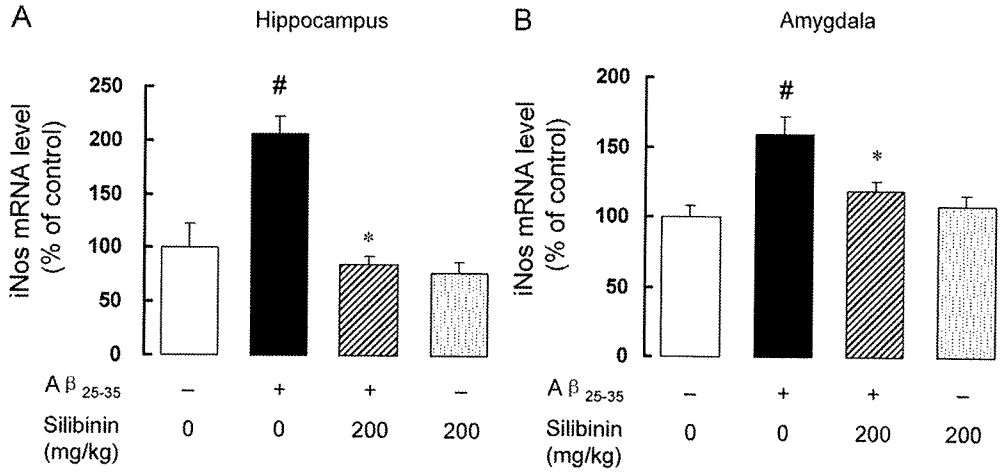

Fig. 4. Effect of silibinin on iNOS mRNA expression in the hippocampus and amygdala of $A\beta_{25-35}$-injected mice. A, hippocampus. B, amygdala. Results were expressed as the mean ± S.E.M. (n = 8), and analyzed by a one-way ANOVA, followed by Tukey's test for multiple comparisons. #, $p <$ 0.05 compared with CMC-treated, distilled water-injected mice; *, $p < 0.05$ compared with CMC-treated, $A\beta_{25-35}$-injected mice.

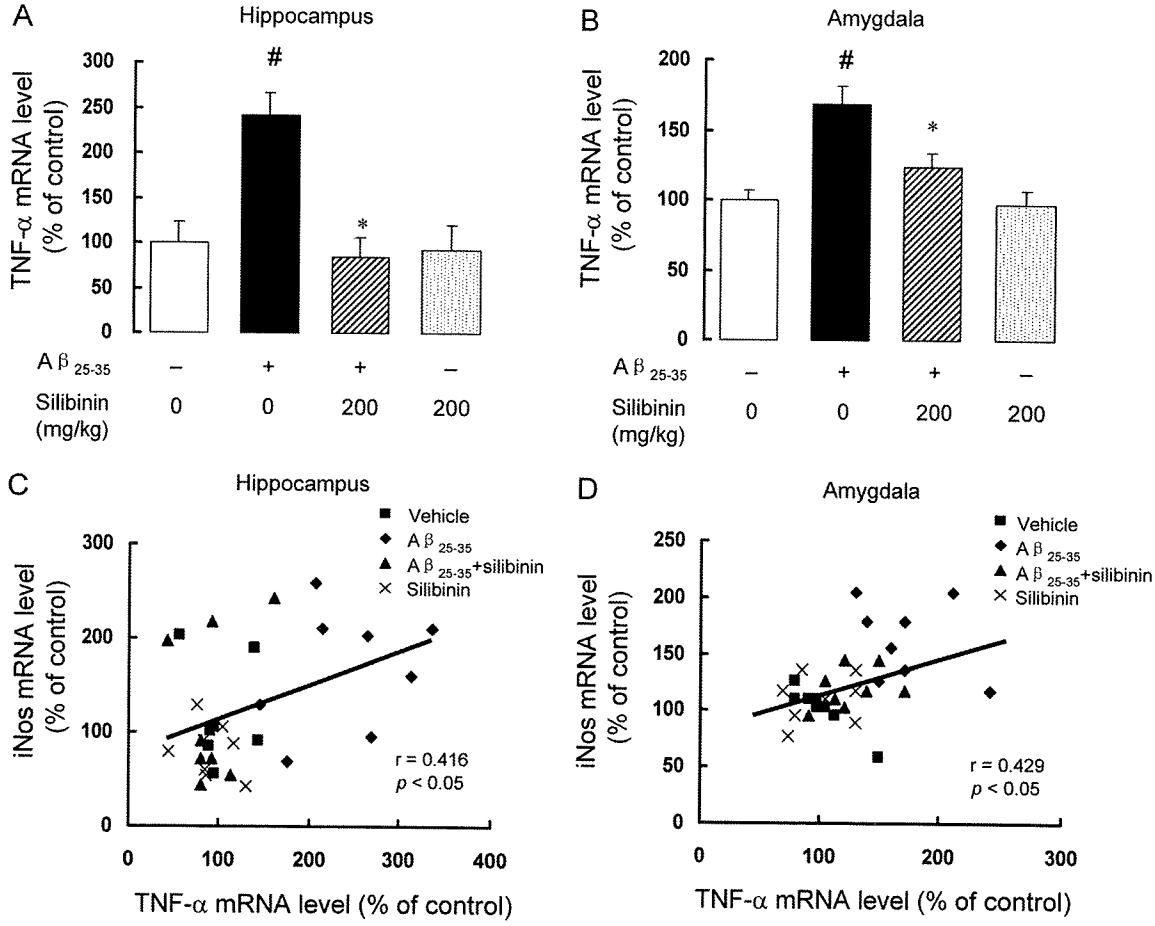

Fig. 5. Effect of silibinin on TNF-α mRNA expression in the hippocampus and amygdala of $A\beta_{25-35}$-injected mice. A and B, TNF-α mRNA expression in the hippocampus (A) and amygdala (B). C and D, correlation of TNF-α mRNA levels with iNOS mRNA levels in the hippocampus (C) and amygdala (D). Results were expressed as the mean ± S.E.M. (n = 8) and analyzed by a one-way ANOVA, followed by Tukey's test for multiple comparisons (A and B) or by a Pearson correlation analysis (C and D). #, $p < 0.05$ compared with CMC-treated, distilled water-injected mice; *, $p < 0.05$ compared with CMC-treated, $A\beta_{25-35}$-injected mice.

significantly attenuated the increase induced by $A\beta_{25-35}$ in both the hippocampus and amygdala [$F(3,31) = 5.55$, $p <$ 0.05, post hoc, $p < 0.05$, Fig. 5A; $F(3,31) = 10.497$, $p < 0.001$, post hoc, $p < 0.05$, Fig. 5B]. Silibinin did not affect TNF-α expression in the hippocampus or amygdala of distilled water-injected mice ($p = 0.994$, Fig. 5A; $p = 0.995$, Fig. 5B). In addition, iNOS mRNA expression correlated with TNF-α mRNA expression in the hippocampus and amygdala (hippocampus: $r = 0.416$, $p < 0.05$, Fig. 5C; amygdala: $r = 0.429$, $p < 0.05$, Fig. 5D).

Discussion

In this study, we demonstrated that silibinin attenuated $A\beta_{25-35}$-induced memory impairment in the cued and contextual fear-conditioning tests and the accumulation of nitroty-

rosine and overexpression of TNF-α and iNOS mRNA in the hippocampus and amygdala. Fear conditioning is a form of memory in which fear is associated with a particular neutral context (e.g., a room) or neutral stimulus (e.g., a tone). Impairment of this type of memory has been found in AD patients (Hamann et al., 2002). Cued and contextual fear-conditioning tests are widely used in experimental animals and have well confirmed that the cued fear response is mainly dependent on the amygdala, whereas the contextual fear response is dependent on the hippocampus and amygdala (Phillips and LeDoux, 1992). In this study, $A\beta_{25-35}$ caused memory impairment in both cued and contextual fear-conditioning tests, and the result consisted with our previous report (Wang et al., 2007). Repeated silibinin treatment significantly attenuated the memory impairment induced by $A\beta_{25-35}$ without affecting the responses to electrical foot shock (flinching, jumping, and vocalization). It is unlikely that the effect of silibinin is due to changes of pain threshold. Furthermore, silibinin itself affected neither motivation nor motor function because our previous study has demonstrated that silibinin had no effect on locomotor activity and exploratory activity (Lu et al., 2009). Taken together, these results suggest that repeated administration of silibinin attenuates the deficit of fear-associative memory induced by $A\beta_{25-35}$.

It has been confirmed that peroxynitrite-mediated damage contributes to Aβ-induced neuronal toxicity and cognitive deficits (Tran et al., 2003; Alkam et al., 2008) and is widespread in the brain of AD patients (Smith et al., 1997). Tyrosine residues are important for redox and cell signaling (Schopfer et al., 2003). Aβ-induced tyrosine nitration, which inhibits the phosphorylation and conformational change of protein, results in memory deficits (Tran et al., 2003; Butterfield et al., 2007). The level of nitrotyrosine has been used as a marker of nitrosative stress and negatively correlated with the level of Aβ in the cerebrum and cognitive function (Smith et al., 1997; Ishii et al., 2000; Tran et al., 2003). In the present study, we found that nitrotyrosine levels in the hippocampus and amygdala negatively correlated with contextual freezing responses. Furthermore, nitrotyrosine level in the amygdala, but not the hippocampus, negatively correlated with the performance in cued conditioning. The result is consistent with previous report that the cued fear response is mainly dependent on the amygdala, whereas the contextual fear response is dependent on both hippocampus and amygdala (Phillips and LeDoux, 1992). It also suggested that the damage of both hippocampus and amygdala contributes to the cognitive deficits induced by Aβ. Moreover, silibinin significantly attenuated the elevation of nitrotyrosine in the hippocampus and amygdala induced by $A\beta_{25-35}$. Our group has demonstrated previously that the activation of iNOS and damage from peroxynitrite contributed to Aβ-induced cognitive deficits in a water-maze test and a novel object recognition test (Tran et al., 2001, 2003; Alkam et al., 2008). These findings suggest that protection from peroxynitrite may be involved in the ameliorating effects of silibinin on cognitive deficits.

Peroxynitrite is produced by superoxides and large amounts of NO synthesized by iNOS under pathological conditions (Reiter et al., 2000). iNOS plays critical roles in Aβ-induced neurotoxicity (Tran et al., 2001, 2003; Alkam et al., 2008) and is up-regulated in the brain of AD patients (Lee et al., 1999). Although the NO synthesized by neuronal NOS facilitates the formation of memories under physiological conditions (Yamada et al., 1995), NO production from iNOS is deleterious under pathological conditions. Because of its independence of elevated intracellular Ca^{2+} levels (Cho et al., 1992), iNOS catalyzes a high-output pathway of NO production (Xie et al., 1999) that is capable of causing neuronal peroxynitrite-mediated damage and dysfunction (Tran et al., 2001, 2003). In the present study, silibinin significantly inhibited the increase in iNOS mRNA in the hippocampus and amygdala induced by $A\beta_{25-35}$. It has been reported that silibinin suppressed the expression or activation of iNOS in several tissues and cell lines, including a glial cell line (Wang et al., 2002). Taken together, it is possible that silibinin prevents $A\beta_{25-35}$-induced peroxynitrite-mediated damage by inhibiting iNOS expression.

The molecular analysis of the iNOS gene has shown the presence of binding sites for nuclear factor-κB and TNF-α-response element in its promoter region (Eberhardt et al., 1996). In this study, we found that silibinin significantly inhibited the increase of TNF-α mRNA in the hippocampus and amygdala induced by $A\beta_{25-35}$. In addition, iNOS mRNA expression correlated with TNF-α mRNA expression in the hippocampus and amygdala. Furthermore, it has been demonstrated in vitro that the stimulation of neuronal cell lines with TNF-α leads to increased expression of inducible nitric-oxide synthase and subsequent apoptosis (Heneka et al., 1998). A specific TNF-α antibody blocked iNOS expression evoked by $A\beta_{1-40}$ in mice (Medeiros et al., 2007). Genetic deletion or pharmacological inhibition of TNF-α suppresses iNOS mRNA expression in the hippocampus and the cognitive deficit induced by $A\beta_{25-35}$ in mice (Alkam et al., 2008). These findings suggested that silibinin inhibits the iNOS expression possibly via down-regulation of TNF-α expression.

Several studies has confirmed that overactivation of glial cells induces TNF-α expression (Combs et al., 2001). Morphological studies have demonstrated that many reactive microglia and astrocytes surround Aβ plaques in the AD brain (Miyazono et al., 1991; McGeer et al., 2006). It is now well documented that fibrillar forms of Aβ serve as a stimulus for glial cell line (Combs et al., 2001; McGeer et al., 2006). It has been reported that silibinin inhibits the microglia activation and overexpression of TNF-α and iNOS evoked by LPS in vitro (Wang et al., 2002). However, whether silibinin regulates the activation of microglia or astrocytes induced by $A\beta_{25-35}$ and the exact molecular targets of silibinin responsible for its antioxidative and anti-inflammatory properties remain unknown.

In addition, silibinin improves antioxidative system (Kren and Walterová, 2005), which may also contribute to its alleviative effect on oxidative damage and cognitive deficits. The delicate balance between oxidative species and antioxidative defenses is disturbed in some pathological conditions such as AD (Guidi et al., 2006). Glutathione (GSH) is an important intracellular antioxidant and responsible for removing oxygen free radical, which is necessary for the formation of peroxynitrite. Previously, we found that silibinin alleviated a reduction in GSH levels induced by $A\beta_{25-35}$ in the hippocampus in this model (Lu et al., 2009). Indeed, silibinin has been reported to increase cellular glutathione content (Valenzuela et al., 1989) and superoxide dismutase levels (Müzes et al., 1991). Therefore, we cannot rule out the possibility that antioxidative systems are involved in alleviative effect of

silibinin on oxidative damage and cognitive deficits induced by $A\beta_{25-35}$.

In conclusion, the present study confirmed that silibinin could ameliorate memory impairment induced by $A\beta_{25-35}$. The effect of silibinin may be attributed to the blocking of inflammatory responses and oxidative stress in the hippocampus and amygdala. As a therapeutic agent, silibinin is well tolerated and largely free of adverse effects, with few negative drug interactions (Jacobs et al., 2002). Therefore, silibinin may be a potential candidate for an AD medication.

Acknowledgments

We thank all of the members in the department of Chemical Pharmacology (Meijo University).

References

Akama KT and Van Eldik LJ (2000) β-Amyloid stimulation of inducible nitric-oxide synthase in astrocytes is interleukin-1β- and tumor necrosis factor-α (TNF-α)-dependent, and involves a TNF-α receptor-associated factor- and NF-κB-inducing kinase-dependent signaling mechanism. *J Biol Chem* **275:**7918–7924.

Alkam T, Nitta A, Mizoguchi H, Saito K, Seshima M, Itoh A, Yamada K, and Nabeshima T (2008) Restraining tumor necrosis factor-α by thalidomide prevents the amyloid β-induced impairment of recognition memory in mice. *Behav Brain Res* **189:**100–106.

Blennow K, de Leon MJ, and Zetterberg H (2006) Alzheimer's disease. *Lancet* **368:**387–403.

Butterfield DA, Reed T, Newman SF, and Sultana R (2007) Roles of amyloid beta-peptide-associated oxidative stress and brain protein modifications in the pathogenesis of Alzheimer's disease and mild cognitive impairment. *Free Radic Biol Med* **43:**658–677.

Cho HJ, Xie QW, Calaycay J, Mumford RA, Swiderek KM, Lee TD, and Nathan C (1992) Calmodulin is a subunit of nitric oxide synthase from macrophages. *J Exp Med* **176:**599–604.

Combs CK, Karlo JC, Kao SC, and Landreth GE (2001) β-Amyloid stimulation of microglia and monocytes results in TNF-α dependent expression of inducible nitric oxide synthase and neuronal apoptosis. *J Neurosci* **21:**1179–1188.

Eberhardt W, Kunz D, Hummel R, and Pfeilschifter J (1996) Molecular cloning of the rat inducible nitric oxide synthase gene promoter. *Biochem Biophys Res Commun* **223:**752–756.

Farfara D, Lifshitz V, and Frenkel D (2008) Neuroprotective and neurotoxic properties of glial cells in the pathogenesis of Alzheimer's disease. *J Cell Mol Med* **12:**762–780.

Fillit H, Ding WH, Buee L, Kalman J, Altstiel L, Lawlor B, and Wolf-Klein G (1991) Elevated circulating tumor necrosis factor levels in Alzheimer's disease. *Neurosci Lett* **129:**318–320.

Guidi I, Galimberti D, Lonati S, Novembrino C, Bamonti F, Tiriticco M, Fenoglio C, Venturelli E, Baron P, Bresolin N, et al. (2006) Oxidative imbalance in patients with mild cognitive impairment and Alzheimer's disease. *Neurobiol Aging* **27:**262–269.

Hamann S, Monarch ES, and Goldstein FC (2002) Impaired fear conditioning in Alzheimer's disease. *Neuropsychologia* **40:**1187–1195.

Heneka MT, Löschmann PA, Gleichmann M, Weller M, Schulz JB, Wüllner U, and Klockgether T (1998) Induction of nitric oxide synthase and nitric oxide-mediated apoptosis in neuronal PC12 cells after stimulation with tumor necrosis factor-alpha/lipopolysaccharide. *J Neurochem* **71:**88–94.

Institute of Laboratory Animal Resources (1996) *Guide for the Care and Use of Laboratory Animals* 7th ed. Institute of Laboratory Animal Resources, Commission on Life Sciences, National Research Council, Washington DC.

Ishii K, Muelhauser F, Liebl U, Picard M, Kühl S, Penke B, Bayer T, Wiessler M, Hennerici M, Beyreuther K, et al. (2000) Subacute NO generation induced by Alzheimer's beta-amyloid in the living brain: reversal by inhibition of the inducible NO synthase. *FASEB J* **14:**1485–1489.

Jacobs BP, Dennehy C, Ramirez G, Sapp J, and Lawrence VA (2002) Milk thistle for the treatment of liver disease: a systematic review and meta-analysis. *Am J Med* **113:**506–515.

Kren V and Walterová D (2005) Silybin and silymarin–new effects and applications. *Biomed Pap Med Fac Univ Palacky Olomouc Czech Repub* **149:**29–41.

Kubo T, Nishimura S, Kumagae Y, and Kaneko I (2002) In vivo conversion of racemized beta-amyloid ([D-Ser 26] Abeta 1–40) to truncated and toxic fragments ([D-Ser 26]Abeta 25–35/40) and fragment presence in the brains of Alzheimer's patients. *J Neurosci Res* **70:**474–483.

La Grange L, Wang M, Watkins R, Ortiz D, Sanchez ME, Konst J, Lee C, and Reyes E (1999) Protective effects of the flavonoid mixture, silymarin, on fetal rat brain and liver. *J Ethnopharmacol* **65:**53–61.

Lee SC, Zhao ML, Hirano A, and Dickson DW (1999) Inducible nitric oxide synthase immunoreactivity in the Alzheimer disease hippocampus: association with Hirano bodies, neurofibrillary tangles, and senile plaques. *J Neuropathol Exp Neurol* **58:**1163–1169.

Lu P, Mamiya T, Lu LL, Mouri A, Zou L, Nagai T, Hiramatsu M, Ikejima T, and Nabeshima T (2009) Silibinin prevents amyloid β peptide-induced memory impairment and oxidative stress in mice. *Br J Pharmacol* **157:**1270–1277.

Maurice T, Lockhart BP, and Privat A (1996) Amnesia induced in mice by centrally administered β-amyloid peptides involves cholinergic dysfunction. *Brain Res* **706:**181–193.

McGeer PL, Rogers J, and McGeer EG (2006) Inflammation, anti-inflammatory agents and Alzheimer disease: the last 12 years. *J Alzheimers Dis* **9:**271–276.

Medeiros R, Prediger RD, Passos GF, Pandolfo P, Duarte FS, Franco JL, Dafre AL, Di Giunta G, Figueiredo CP, Takahashi RN, et al. (2007) Connecting TNF-alpha signaling pathways to iNOS expression in a mouse model of Alzheimer's disease: relevance for the behavioral and synaptic deficits induced by amyloid beta protein. *J Neurosci* **27:**5394–5404.

Miyazono M, Iwaki T, Kitamoto T, Kaneko Y, Doh-ura K, and Tateishi J (1991) A comparative immunohistochemical study of kuru and senile plaques with a special reference to glial reactions at various stages of amyloid plaque formation. *Am J Pathol* **139:**589–598.

Müzes G, Deák G, Láng I, Nékám K, Gergely P, and Fehér J (1991) Effect of the bioflavonoid silymarin on the in vitro activity and expression of superoxide dismutase (SOD) enzyme. *Acta Physiol Hung* **78:**3–9.

Perry RT, Collins JS, Wiener H, Acton R, and Go RC (2001) The role of TNF and its receptors in Alzheimer's disease. *Neurobiol Aging* **22:**873–883.

Phillips RG and LeDoux JE (1992) Differential contribution of amygdala and hippocampus to cued and contextual fear conditioning. *Behav Neurosci* **106:**274–285.

Pike CJ, Walencewicz-Wasserman AJ, Kosmoski J, Cribbs DH, Glabe CG, and Cotman CW (1995) Structure-activity analyses of β-amyloid peptides: contributions of the β25–35 region to aggregation and neurotoxicity. *J Neurochem* **64:**253–265.

Reiter CD, Teng RJ, and Beckman JS (2000) Superoxide reacts with nitric oxide to nitrate tyrosine at physiological pH via peroxynitrite. *J Biol Chem* **275:**32460–32466.

Schopfer FJ, Baker PR, and Freeman BA (2003) NO-dependent protein nitration: a cell signaling event or an oxidative inflammatory response? *Trends Biochem Sci* **28:**646–654.

Smith MA, Richey Harris PL, Sayre LM, Beckman JS, and Perry G (1997) Widespread peroxynitrite-mediated damage in Alzheimer's disease. *J Neurosci* **17:**2653–2657.

Tran MH, Yamada K, Nakajima A, Mizuno M, He J, Kamei H, and Nabeshima T (2003) Tyrosine nitration of a synaptic protein synaptophysin contributes to amyloid beta-peptide-induced cholinergic dysfunction. *Mol Psychiatry* **8:**407–412.

Tran MH, Yamada K, Olariu A, Mizuno M, Ren XH, and Nabeshima T (2001) Amyloid beta-peptide induces nitric oxide production in rat hippocampus: association with cholinergic dysfunction and amelioration by inducible nitric oxide synthase inhibitors. *FASEB J* **15:**1407–1409.

Valenzuela A, Aspillaga M, Vial S, and Guerra R (1989) Selectivity of silymarin on the increase of the glutathione content in different tissues of the rat. *Planta Med* **5:**420–422.

Wada R, Tifft CJ, and Proia RL (2000) Microglial activation precedes acute neurodegeneration in Sandhoff disease and is suppressed by bone marrow transplantation. *Proc Natl Acad Sci U S A* **97:**10954–10959.

Walsh DM and Selkoe DJ (2004) Deciphering the molecular basis of memory failure in Alzheimer's disease. *Neuron* **44:**181–193.

Wang D, Noda Y, Zhou Y, Mouri A, Mizoguchi H, Nitta A, Chen W, and Nabeshima T (2007) The allosteric potentiation of nicotinic acetylcholine receptors by galantamine ameliorates the cognitive dysfunction in beta amyloid 25–35 i.c.v.-injected mice: involvement of dopaminergic systems. *Neuropsychopharmacology* **32:**1261–1271.

Wang MJ, Lin WW, Chen HL, Chang YH, Ou HC, Kuo JS, Hong JS, and Jeng KC (2002) Silymarin protects dopaminergic neurons against lipopolysaccharide-induced neurotoxicity by inhibiting microglia activation. *Eur J Neurosci* **16:**2103–2112.

Xie QW, Cho HJ, Calaycay J, Mumford RA, Swiderek KM, Lee TD, Ding A, Troso T, and Nathan C (1999) Cloning and characterization of inducible nitric oxide synthase from mouse macrophages. *Science* **256:**225–228.

Yamada K, Noda Y, Nakayama S, Komori Y, Sugihara H, Hasegawa T, and Nabeshima T (1995) Role of nitric oxide in learning and memory and in monoamine metabolism in the rat brain. *Br J Pharmacol* **115:**852–858.

Address correspondence to: Dr. Toshitaka Nabeshima, Department of Chemical Pharmacology, Graduate School of Pharmaceutical Sciences, Meijo University, 150 Yagotoyama, Tempaku-ku, Nagoya 468-8503, Japan. E-mail: tnabeshi@ccmfs.meijo-u.ac.jp

nature genetics

Usp46 is a quantitative trait gene regulating mouse immobile behavior in the tail suspension and forced swimming tests

Shigeru Tomida[1], Takayoshi Mamiya[2], Hirotake Sakamaki[1], Masami Miura[3], Toshihiko Aosaki[3], Masao Masuda[3], Minae Niwa[2], Tsutomu Kameyama[4], Junya Kobayashi[1], Yuka Iwaki[1], Saki Imai[1], Akira Ishikawa[5], Kuniya Abe[6], Takashi Yoshimura[1], Toshitaka Nabeshima[2] & Shizufumi Ebihara[1]

The tail suspension test (TST) and forced swimming test (FST) are widely used for assessing antidepressant activity and depression-like behavior. We found that CS mice show negligible immobility in inescapable situations. Quantitative trait locus (QTL) mapping using CS and C57BL/6J mice revealed significant QTLs on chromosomes 4 (FST) and 5 (TST and FST). To identify the quantitative trait gene on chromosome 5, we narrowed the QTL interval to 0.5 Mb using several congenic and subcongenic strains. Ubiquitin-specific peptidase 46 (*Usp46*) with a lysine codon deletion was located in this region. This deletion affected nest building, muscimol-induced righting reflex and anti-immobility effects of imipramine. The muscimol-induced current in the hippocampal CA1 pyramidal neurons and hippocampal expression of the 67-kDa isoform of glutamic acid decarboxylase were significantly decreased in the *Usp46* mutant mice compared to control mice. These phenotypes were rescued in transgenic mice with bacterial artificial chromosomes containing wild-type *Usp46*. Thus, *Usp46* affects the immobility in the TST and FST, and it is implicated in the regulation of GABA action.

The TST and FST have been recognized as useful experimental paradigms for assessing antidepressant activity and depression-like behavior. In these tests, animals are subjected to the short-term, inescapable stress of being suspended by their tail or being forced to swim in a water-filled cylinder. In such situations, the animals rapidly adopt a characteristic immobile posture that has been named "behavioral despair" on the assumption that the animals have given up hope of escaping[1,2]. These tests have been widely used for screening drugs for antidepressant activity and in preclinical depression studies for understanding the underlying pathophysiology of affective disorders, particularly for assessing depression-related behavior in genetically modified mice[3,4].

Several mental illnesses such as affective disorders or schizophrenia are thought to arise from naturally occurring variant genes and their interactions, and from gene-environment interactions in which each gene confers subtle effects on the appearance of the diseases. In the absence of such interactions, the disease risk elicited by each variant gene is low but increases with an appropriate combination of genetic and environmental factors. Because diseases elicited by single gene defects are fairly rare, QTL analysis has been extensively performed in animal models to dissect such complex traits[5]. However, these attempts have hardly been successful, and $<1\%$ of QTLs (only approximately 20 genes) have been identified in mice and rats[6]. In recent years, several QTL studies have been conducted in mice on the basal immobility time and antidepressant response in the TST and FST[7–11]. These studies have resulted in the mapping of many QTLs, and several candidate genes underlying these behaviors have been proposed; however, so far investigators have not identified any genes as responsible for these behaviors.

The CS mouse is an inbred strain originally established by the hybridization of the NBC and SII strains, which are both now extinct. CS mice exhibit several distinct phenotypes of circadian behavioral rhythms, such as a long free-running period, spontaneous rhythm splitting and entrainment of circadian rhythms in response to a daily restricted feeding schedule under constant darkness[12–14]. In addition, the sleep properties of CS mice are distinct from those of C57BL/6J and C3H/He mice, which have normal circadian rhythms[15]. Because many mental illnesses are associated with abnormalities in the circadian system and sleep patterns, we characterized the behavioral phenotypes in CS mice with a battery of behavioral tests. Among these phenotypes, we found that CS mice show an extremely low immobility time (almost no immobility) in both the TST and FST, which

[1]Division of Biomodeling, Graduate School of Bioagricultural Sciences, Nagoya University, Furo-cho, Chikusa-ku, Nagoya, Japan. [2]Department of Chemical Pharmacology, Faculty of Pharmacy, Meijo University, Tempaku-ku, Nagoya, Japan. [3]Neural Circuits Dynamics Research Group, Tokyo Metropolitan Institute of Gerontology, Itabashi-ku, Tokyo, Japan. [4]Japan Institute of Psychopharmacology, Higashi-ku, Nagoya, Japan. [5]Division of Applied Genetics and Physiology, Graduate School of Bioagricultural Sciences, Nagoya University, Furo-cho, Chikusa-ku, Nagoya, Japan. [6]RIKEN BioResource Center, Technology and Development Team for Mammalian Cellular Dynamics, Tsukuba, Japan. Correspondence should be addressed to S.E. (ebihara@agr.nagoya-u.ac.jp).

Received 10 June 2008; accepted 2 February 2009; published online 24 May 2009; doi:10.1038/ng.344

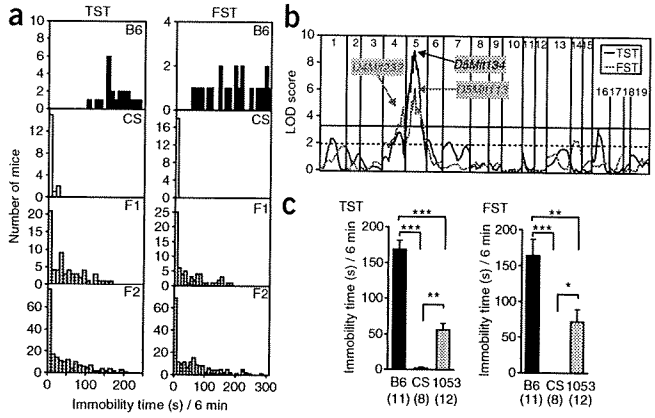

Figure 1 Linkage analysis and phenotypes of the chromosome 5 congenic strain. (**a**) Frequency histograms of the immobility time in the tail suspension test (TST) and the forced swimming test (FST) for parental, F_1 and F_2 mice. (**b**) Genome-wide linkage analysis for the immobility time on TST and FST using Map Manager QTXb20. Three significant QTLs were mapped with a peak at *D5Mit134* on TST and at *D4Mit232* and *D5Mit113* on FST. The solid and dotted lines indicate the significance level (LOD score = 3.30 on both TST and FST) and suggestive level (LOD score = 1.95 on both TST and FST), respectively. (**c**) TST and FST immobility time (mean ± s.e.m.) in B6, CS and B6.CS-Ngu1053 male mice. The CS and B6.CS-Ngu1053 mice showed a significantly shorter immobility time than the B6 mice on both TST and FST (one-way ANOVA: TST, $F_{2,28} = 46.3$, $P < 9.4 \times 10^{-10}$; FST, $F_{2,28} = 18.8$, $P < 6.6 \times 10^{-6}$; Tukey-Kramer *post hoc* test: $^{***}P < 0.001$, $^{**}P < 0.01$, $^{*}P < 0.05$). The number of mice used is shown within parentheses.

prompted us to undertake QTL genetic analysis to identify the responsible gene. By using a forward genetic approach[6,16,17], we succeeded in identifying the responsible gene. Here, we report that the gene encoding ubiquitin-specific peptidase 46 (*Usp46*) is one of the quantitative trait genes that cause such behaviors.

RESULTS

Behavioral phenotyping of the C57BL/6J and CS strains

To assess the behavioral characteristics of the CS strain, we subjected C57BL/6J (B6) and CS mice to a battery of behavioral tests, including the open-field, light-dark exploration, elevated plus-maze, prepulse inhibition, Y-maze, tail suspension and forced swimming tests (**Supplementary Table 1** online).

The open-field test is widely used to quantitate overall activity and anxiety-related behavior, although this test is not so specific for anxiety-related behavior[18]. In this test, the ambulatory activity was significantly lower in the CS mice than in the B6 mice ($P < 0.01$, Student's *t*-test), but no differences were observed in the other phenotypes (grooming, rearing and defecation). In the light-dark box test, which is primarily used to detect anxiolytic-like or anxiogenic-like activity of a drug[19], the CS mice spent significantly less time ($P < 0.01$, Student's *t*-test) in the dark compartment and defecated more frequently ($P < 0.01$, Mann-Whitney *U* test) than the B6 mice, although there were no significant differences in the time of light-dark transitions between the two compartments. In the elevated plus-maze test, which is also used to detect anxiolytic-like behavior[20], no significant differences were observed in the time spent on the open arm between the two strains; however, the CS mice defecated more frequently ($P < 0.001$, Student's *t*-test) than the B6 mice. The prepulse inhibition test, in which a weak prestimulus or prepulse suppresses the response to a startling stimulus, is used to evaluate sensorimotor gating, and it is thought that deficits in this response represent biological markers for schizophrenia[20,21]. In this test and in the Y-maze test, which is considered to reflect the status of short-term and working memory in humans[22], there were no significant differences between the two strains. In contrast to the above-mentioned phenotypes, the results in the TST and FST were unusual in the CS mice, which showed negligible immobility throughout the test period.

QTL analysis

To map the genes responsible for the aberrant immobility of CS mice observed in the TST and FST, we genotyped 203 F_2 mice produced by intercrossing F_1 mice obtained from B6 and CS mice; interval mapping was performed using Map Manager QTXb20 followed by nonparametric interval mapping using R/qtl (http://www.rqtl.org/). Consequently, we detected significant QTLs in the TST (likelihood of odds score (LOD) 8.90, QTXb20; LOD 8.92, R/qtl) and FST (LOD 6.08, QTXb20; LOD 6.92, R/qtl) on chromosome 5, and only in the FST (LOD 4.71, QTXb20; LOD 4.09, R/qtl) on chromosome 4 (**Fig. 1a,b**; **Supplementary Fig. 1** and **Supplementary Tables 2** and **3** online). The peak positions of the QTLs on chromosome 5 for immobility in the TST and FST were similar (TST: 29 cM for QTXb20, 28 cM for R/qtl; FST: 30 cM for QTXb20, 30 cM for R/qtl). In addition, suggestive QTLs were detected on chromosomes 1, 4, 6, 7 and 16 in the TST and on chromosome 14 in the FST by QTXb20, and on chromosomes 4, 6, 7 and 16 in the TST and on chromosomes 1, 6 and 14 in the FST by R/qtl (**Supplementary Tables 2** and **3**). To detect epistatic interactions, we performed two-locus interaction analysis for all possible markers using QTXb20. However, we could not find any pair of markers that significantly affected the immobility time in the TST and FST ($P > 0.05$).

Reducing the QTL interval

To reduce the QTL interval on chromosome 5, we developed a number of congenic or subcongenic strains by crossing CS as the donor strain with B6 as the recipient strain using a "speed-congenic" approach (**Supplementary Fig. 2** online). The B6.CS-Ngu1053 strain, which was subsequently used in different experiments, carried homozygous CS alleles within its congenic interval (an approximately 16-Mb region from *D5B6CS85* to *D5Mit259*) on a B6 genetic background. To validate QTL linkage analysis, we subjected the B6.CS-Ngu1053 strain to TST and FST and found that the immobility time of this strain was significantly shorter than that of the B6 strain in both the TST and the FST; however, its immobility time was longer than that of CS in both the tests (TST: $P < 0.001$ versus B6, $P < 0.01$ versus CS; FST: $P < 0.01$ versus B6, $P < 0.05$ versus CS) (**Fig. 1c**).

To narrow down the critical interval that harbors the responsible gene, we generated two subcongenic strains by crossing B6.CS-Ngu1053 with B6. The B6.CS-Ngu2271 strain contained an approximately 0.5-Mb nonoverlapping region with the B6.CS-Ngu1053 strain at the centromeric side, whereas the B6.CS-Ngu3042 strain carried a nonoverlapping region at the telomeric side (**Fig. 2a**). The B6.CS-Ngu2271 strain showed almost the same TST immobility time as B6, which indicates that the 0.5-Mb nonoverlapping region represents the critical interval. The shorter immobility time of the B6.CS-Ngu3042 strain supports the notion that the responsible quantitative trait gene is located in this interval.